Max-Planck-Institut
für Meteorologie

REPORT No. 109

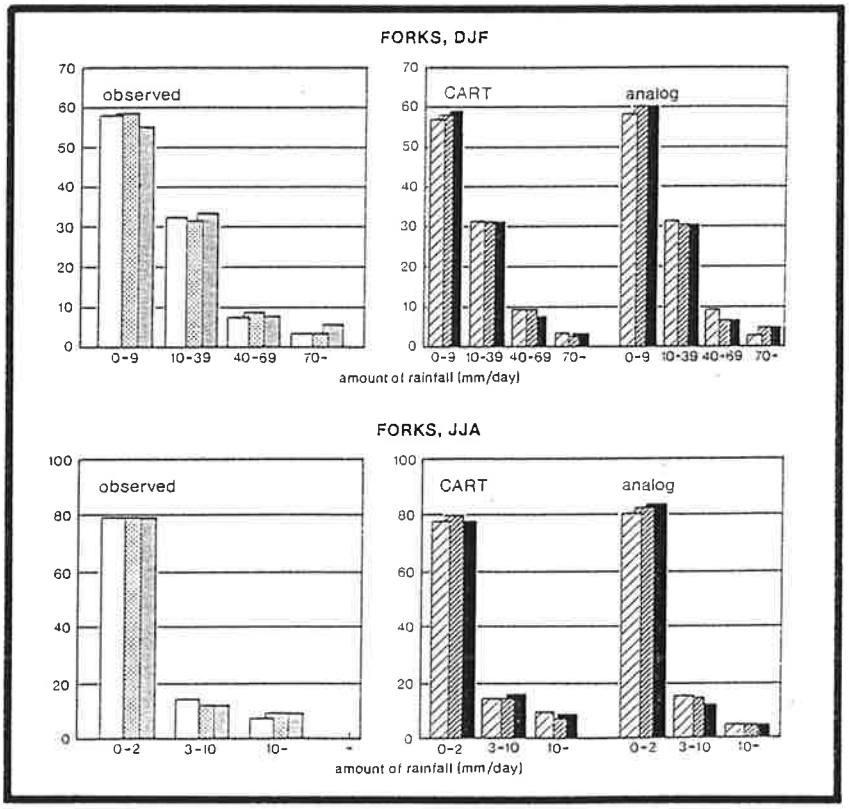

STOCHASTIC CHARACTERIZATION OF REGIONAL CIRCULATION PATTERNS FOR CLIMATE MODEL DIAGNOSIS AND ESTIMATION OF LOCAL PRECIPITATION

von

EDUARDO ZORITA • JAMES P. HUGHES
DENNIS P. LETTEMAIER • HANS VON STORCH

Hamburg, August 1993

AUTHORS:

Eduardo Zorita
Hans von Storch

Max–Planck–Institut
für Meteorologie

James P. Hughes

Deparment of Statistics
University of Washington
Seattle
Washington
U.S.A.

Dennis P. Lettemaier

Department of Civil Engineering
University of Washington
Seattle
Washington
U.S.A.

MAX–PLANCK–INSTITUT
FÜR METEOROLOGIE
BUNDESSTRASSE 55
D–20146 Hamburg
F.R. GERMANY

Tel.: +49 (40) 4 11 73–0
Telex: 211092 mpime d
Telemail: MPI.METEOROLOGY
Telefax: +49 (40) 4 11 73–298

REPb 109

Stochastic characterization of regional circulation patterns for climate model diagnosis and estimation of local precipitation

EDUARDO ZORITA
Max-Planck-Institut für Meteorologie, Hamburg, Germany

JAMES P. HUGHES
Department of Statistics, University of Washington, Seattle, Washington

DENNIS P. LETTEMAIER
Department of Civil Engineering, University of Washington, Seattle, Washington

HANS v. STORCH
Max-Planck-Institut für Meteorologie, Hamburg, Germany

ABSTRACT

Two statistical approaches for linking large-scale atmospheric circulation patterns and daily local rainfall are described and applied to several GCM (general circulation model) climate simulations. The ultimate objective is to simulate local precipitation associated with alternative climates. The index stations are located near the West and East North American coasts. The first method is based on CART analysis (Classification and Regression trees). It finds the classification of observed daily SLP (sea level pressure) fields in weather types that are most strongly associated with the presence/absence of rainfall in a set of index stations. The best results were obtained for winter rainfall for the West Coast, where a set of physically reasonable weather types could be identified, whereas for the East Coast the rainfall process seemed to be spatially less coherent. The GCM simulations were validated against observations in terms of probability of occurrence and survival time of these weather states. Some discrepancies werefound but there was no systematic bias, indicating that this behavior depends on the particular dynamics of each model. This classification method was then used for the generation of daily rainfall time series from the daily SLP fields from historical observation and from the GCM simulations Whereas the mean rainfall and probability distributions were rather well replicated, the simulated dry periods were in all cases shorter than in the rainfall observations. The second rainfall generator is based on the analog method and uses information on the evolution of the SLP field in several previous days. It was found to perform reasonably well, although some downward bias in the simulated rainfall persistence was still present. Rainfall changes in a $2xCO_2$ climate were investigated by applying both methods to the output of a greenhouse-gas experiment. The simulated precipitation changes were small.

---

1. Introduction.

One of the largest uncertainties in climate simulations produced by the present generation of general circulation models (GCMs) is the hydrological cycle at the land surface (Chahine, 1992). The physical processes that contribute to the atmospheric and surface hydrologic cycles, such as cloud formation, precipitation, infiltration, evaporation, and runoff production, evolve over a much smaller scale than the resolution of today's GCMs, which are limited by computational considerations to a typical range of 200 to 1000 km. Therefore, these process have to be incorporated into the GCMs by means of parameterizations, which may introduce additional errors in the GCM simulations (Thomas and Henderson-Sellers, 1991). On the other hand, changes in the hydrological cycle caused by an increase of atmospheric greenhouse gases could have a considerable societal impact (Rind, 1992), so that there is a need for assessment of the

ISSN 0937–1060

potential effects of climate change at scales that cannot be resolved by current GCMs (Grotz and MacCracken, 1991). Essentially two strategies have been suggested to overcome this scale mismatch (e.g., Giorgi and O'Mearns, 1991). The first is to develop finer-resolution regional climate models that are driven by boundary conditions simulated by global GCMs at coarser scales (Giorgi, 1990). In theory, these nested models should be able to replicate the physical processes operating at regional scales and can take into account orographic features that are partially or totally absent in a GCM and that may be important for regional climates. This approach is, however, computationally costly, and the present practically attainable resolution using this approach requires that some processes still must be parameterized. Another problem with this approach is that feedbacks from the regional model into the GCM are not incorporated. While alternative numerical schemes such as the adaptive multigrid method could allow such feedbacks to be modeled (see, for example, Barros and Lettenmaier, 1992) these schemes have not yet been applied to GCMs.

Another possibility is to derive statistical models from the observed relationships between the large-scale atmospheric fields, such as sea level pressure (SLP) or geopotential heights, and local variables, such as precipitation or surface temperature.Once the statistical model parameters are estimated from a training set of large-scale and local observations, the models may be used to infer changes in the local variables due to changes in the large-scale fields simulated from GCM sensitivity experiments. For instance, multiple regression equations linking the 700 mb geopotential heights and precipitation (Klein and Bloom, 1988) and geopotential heights and fire weather elements (Klein and Whistler, 1990) have been used in the U.S. Wigley et al. (1990) used, among other variables, large-scale spatial averages of near-surface temperature and correlated them with local temperature time series. With a slightly different strategy Karl et al.(1990) used a modified Model Output Statistics technique to identify relationships between a set of free atmosphere variables as predictors and near-surface temperature and precipitation as predictands. Von Storch et al. (1993) used canonical correlation analysis to relate local monthly precipitation to the SLP field. These studies have all concluded that local climate changei nferred directly from GCM simulations interpolated to the local scale may differ markedly from local simulations derived from the statistical approach.

All of the statistical techniques noted above essentially make use of correlations between the time series of the large-scale and local variables. However there are some important variables that are discontinuous in time,like daily precipitation, and are not suitable for statistical techniques such as regression-based methods. On the other hand there are whole families of sector models (for prediction of agricultural production, hydroelectric power production, surface water supply, terrestrial and aquatic ecosystems, to mention a few), which require as input local precipitation amounts at daily or near-daily time scales. In this case statistical models have to be based upon other techniques, such as the use of weather classification schemes applied to an altered climate can then be generated by classifying the GCM-simulated large-scale fields as belonging to a weather state (type) and sampling the local observations from days belonging to this weather state. Bardossy and Plate (1991) made use of such a strategy bclassification scheme traditionally used by the German Weather Service. Wilson et al (1992) defined weather states through a combined Principal Components Analysis of sea level pressure, 850 mb temperature and 850 mb geopotential height. Hughes at al (1993) applied Classification and Regression Tree (CART) analysis to identify the weather types that were most related to occurrence or absence of precipitation.

At least three assumptions underlie this type of statistical strategy. First, the GCMs are assumed to be able to simulate realistically the large-scale atmospheric features that give rise to the observed distribution of regional climates, such as the subtropical highs, subpolar lows, and storm tracks. Second, the relationships between the large-scale and local variables are assumed to hold under the

altered climate. Third, the statistical procedure to estimate the local variable should be able to replicate the historical data, or at least important aspects of their statistical behavior, when it is driven with the observed large-scale circulation.

This paper fits within the framework of this coupled empirical/statistical approach. Its aim is to check to what extent some of the above assumptions are fulfilled in practice and to help establish the degree of confidence that can be placed in these procedures. The applications of the method are for daily rainfall at selected stations in two North American regions at mid-latitudes, the Columbia River basin, located near the West Coast, and the middle-Atlantic region of the eastern U.S. With this goal in mind we first analyze two present-climate simulations of the General Circulation Models of the Geophysical Fluid Dynamics Laboratory (GFDL), and the Max Planck Institute of Meteorology (MPI) respectively. In Section 2 the regional performance of the control runs of two GCMs is examined. For this purpose the simulated long-term mean SLP field, its standard deviation and its coherent patterns of variability (empirical orthogonal functions) are compared to the corresponding patterns derived from observations. One of the statistical models used to generate daily rainfall at the selected stations is based on a circulation-type classification by CART analysis, that was used by Hughes et al (1993). It is applied in this paper to historical SLP and rainfall data in the Columbia River basin and middle-Atlantic regions, and is used to identify the circulation types that are most strongly related to rainfall at the selected stations. Although not strictly essential to assess the quality of the downscaling procedure, it is of interest to validate the two GCM control runs in terms of the circulation types, by computing quantities like probability of occurrence and lifetimes of each weather state and how these change in a $2xCO_2$ experiment performed with the MPI model. This is described in Sections 4 and 5 of the paper.

Finally, in Section 6, the circulation types identified by CART analysis (Hughes et al, 1993) are used for the generation of daily precipitation time series at individual stations. For this purpose the historical SLP fields, as well as the ones simulated by the GFDL and MPI GCMs are used tosimulate some important statistical properties of the rainfall time series. One important deficiency of this method, as noted by Hughes et al (1993), is that precipitation sequences generated from the observed SLP fields were not as persistent in terms of the occurrence or absence of precipitation was not as persistent as the observations. Hughes et al explored a modified model that included dependency on precipitation in the previous day, which improved their results. However, in the context of climate change assessment, this modification is not conceptually very satisfactory because it requires the ad-hoc assumption that this dependency will remain unchanged in a new climate. Here we explore the possibility of capturing this higher persistence using the information of the large-scale SLP field alone. The idea is to use not just the SLP field on a certain day but also its evolution over the previous days. For computational reasons CART analysis only accepts a limited number of input variables and therefore another, simpler, stochastic model based on a more traditional analog method is described.

2. Data and statistical techniques

Results from three climate simulations were used in this study. The first was a 10-year control run of the GFDL GCM performed with prescribed sea surface temperatures and interactive clouds. The GFDL model uses a spectral formulation with R30 resolution, approximately equivalent to a regular grid of 3.75 degrees longitude x 2.22 degrees latitude. The second experiment wa a control run of the MPI coupled ocean-atmosphere model (Cubasch et al, 1991).The atmospheric part of this climate model (Roeckner et al, 1989) is also a spectral model with a T21 resolution (about 5.62 x 5.62 degrees). The third experiment was a $2xCO_2$ run with the MPI model. In this experiment the atmospheric greenhouse gas concentration was doubled from its value in the control run. Daily means of the SLP pressure field between years 76 and 100 of these two MPI simulations were used.

Twenty years of daily SLP analyses from the US National Meteorological Center (NMC), for the period 1965 to 1984 were used in this study.

These data were retrieved from a CD prepared by the Department of Atmospheric Sciences of the University of Washington (Mass et al., 1987) and interpolated to a rectangular latitude-longitude grid from the NMC octogonal grid, using software developed at NCAR. Infrequent missing data were filled in by interpolation between the previous and following days. All data were interpolated to the lowest resolution T21 to avoid possible inconsistencies in the subsequent statistical analysis.

Daily station precipitation data in the period 1965-1984 were retrieved from U.S. National Climatic Data Center records. Gaps in these data were removed by using information from nearby stations via a prorating method (Wallis et al., 1991). The station positions are indicated in Fig. 1.

Two multivariate statistical techniques were applied to the data sets. Empirical Orthogonal Function analysis (EOF; Preisendorfer, 1988) is often used in climatology to reduce the number of degrees of freedom of large-scale anomaly fields, by identifying a limited number of variables that can describe most of the variance. Mathematically this is achieved by diagonalizing the cross-covariance matrix calculated between anomalies at grid nodes. The eigenvectors of this matrix are called EOF loadings and the variance explained by the EOF is given by its associated eigenvalue. Each EOF has an associated time series (also known as scores) that describes the time evolution of the EOF and that can be calculated at each time step by projecting the EOF onto the field. Since the normalizing constant for each EOF is not defined (as for all eigenvectors of any matrix) we choose this constant in such a way that the associated time series has standard deviation unity (with no physical units), so that the physical units are carried by the EOF. One important property of the scores is that the correlation between any pair of them is zero.

The second statistical technique used was Classification and Regression Tree (CART) analysis (Breiman et al, 1984). This technique provides an objective way to define a scheme to classify the daily circulation in a small number of weather classes, which are relevant for the precipitation occurrence or absence at a certain set of stations (precipitation is considered here as a two-valued discrete variable, wet or dry). The daily circulation states are classified by means of a binary decision tree, the nodes of which are split depending on the values of one of the input variables, such as, for instance, the value of the SLP field at a certain grid node or some other large-scale circulation index. Each terminal node of the decision tree corresponds to a weather state. The decision tree that results from the CART analysis has the property that the joint precipitation occurrence probability distributions corresponding to the different weather states are, in a certain sense, maximally separated.

3. Regional model validation.

In this section some basic statistical parameters derived from the control runs of the two GCMs are compared with the same parameters derived from the NMC data. This comparison will be restricted to sea level pressure in the two regions of interest, the west (region from latitude 30 -70 N, 115 -180 W) and east (30 -70 N , 45 -100 W) North American coasts at mid-latitudes for winter and summer. All of the analyses are based on daily data, in the case of the NMC observations, taken at 0000 GMT.

Fig. 2 shows the long term mean of the SLP field in January and July for the observations and the two model runs for the western region. In January, both models produce a stronger Aleutian Low than is observed in the historical data. In the GFDL run the low is centered northeast of its correct position. In July the MPI control run correctly reproduces the summer high pressure cell over the Pacific Ocean, whereas in the GFDL run the high pressure is much stronger than in the observations. The long-term standard deviation of the SLP fields calculated from the daily means for January and July are shown in Fig 3. The historical data for January show a broad variability maximum centered over the Aleutian islands. In the MPI run this maximum is fairly well simulated. The GFDL model tends to be much more variable than the observations, with its maximum extending eastward into the continent. In July the variability of

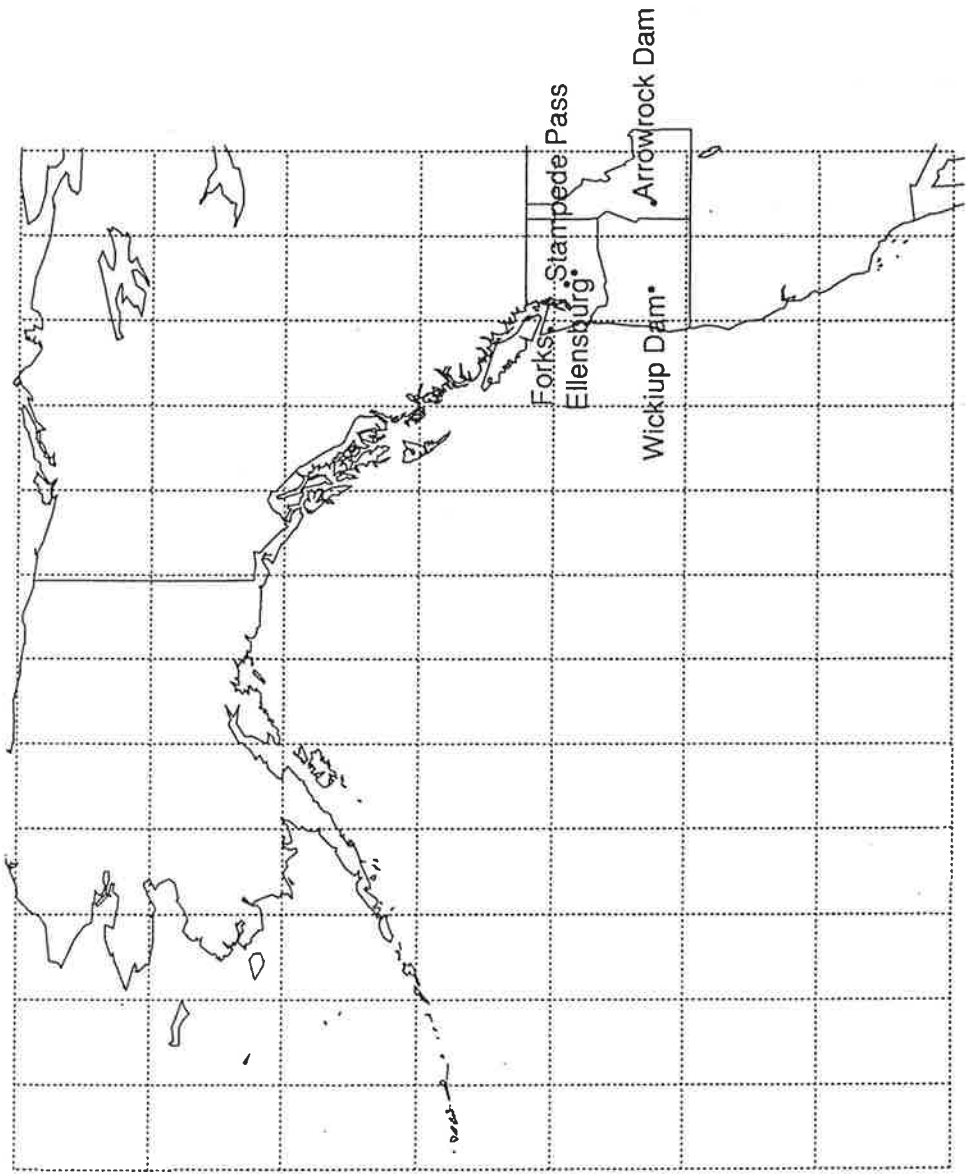

Figure 1. Positions of the stations used in this paper.

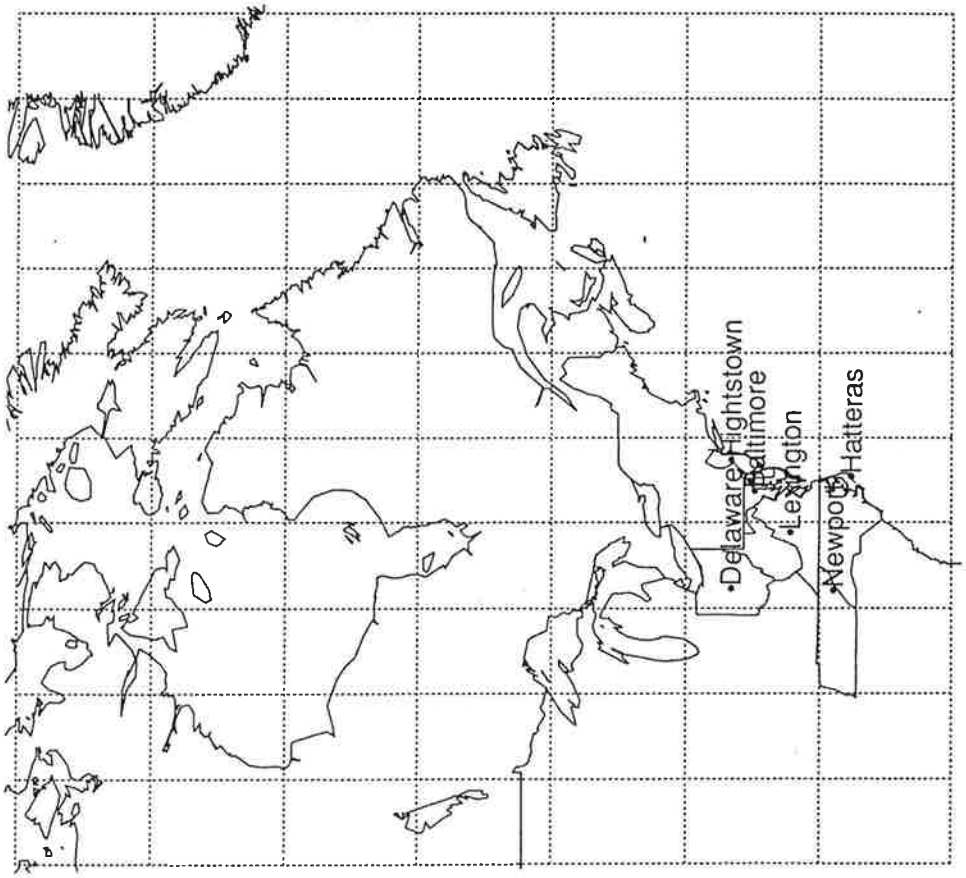

Figure 1 (cont).

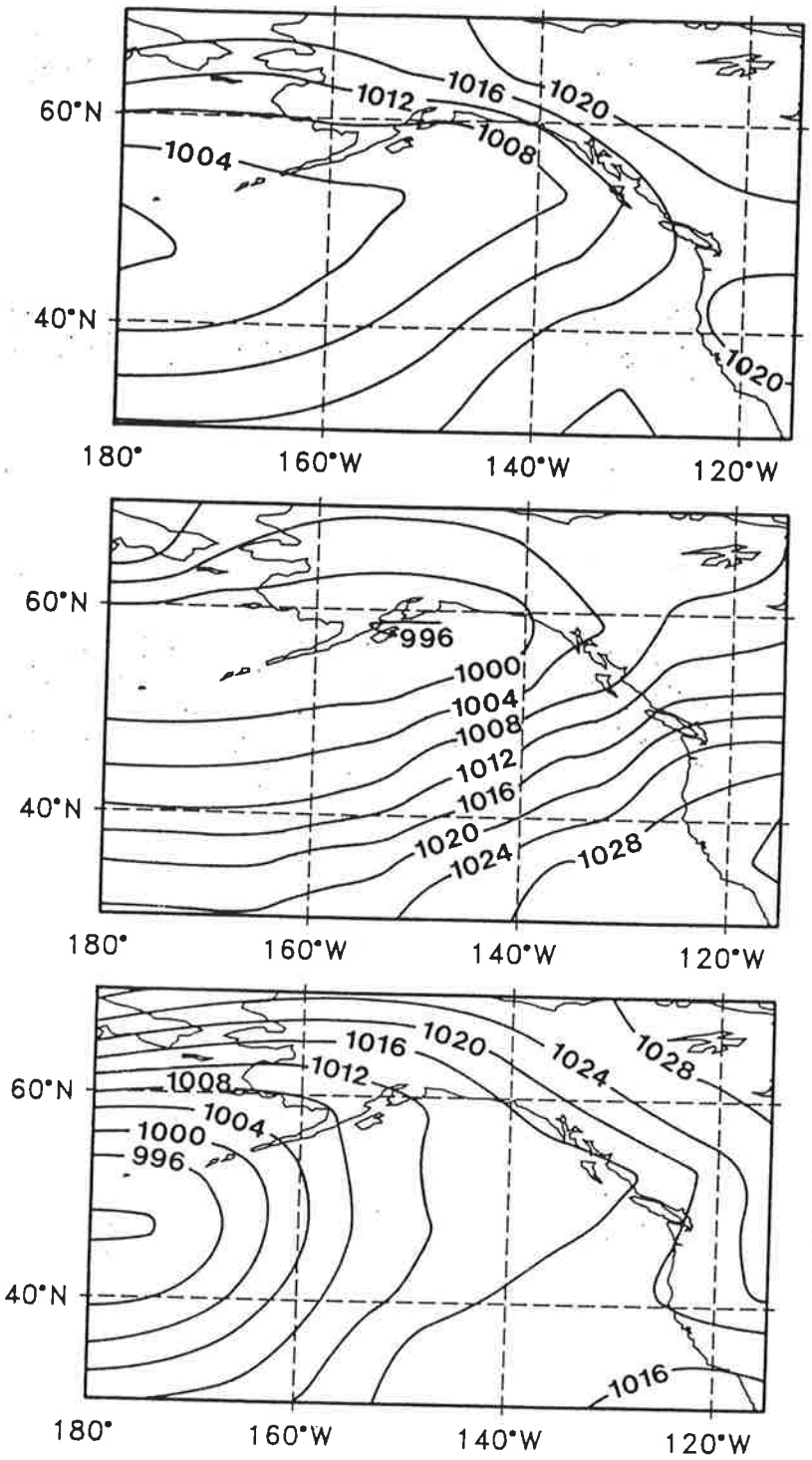

Figure 2. Mean SLP fields (mb) in the Pacific-North American sector as derived from the NMC analysis, the GFDL model and the MPI model: a) January

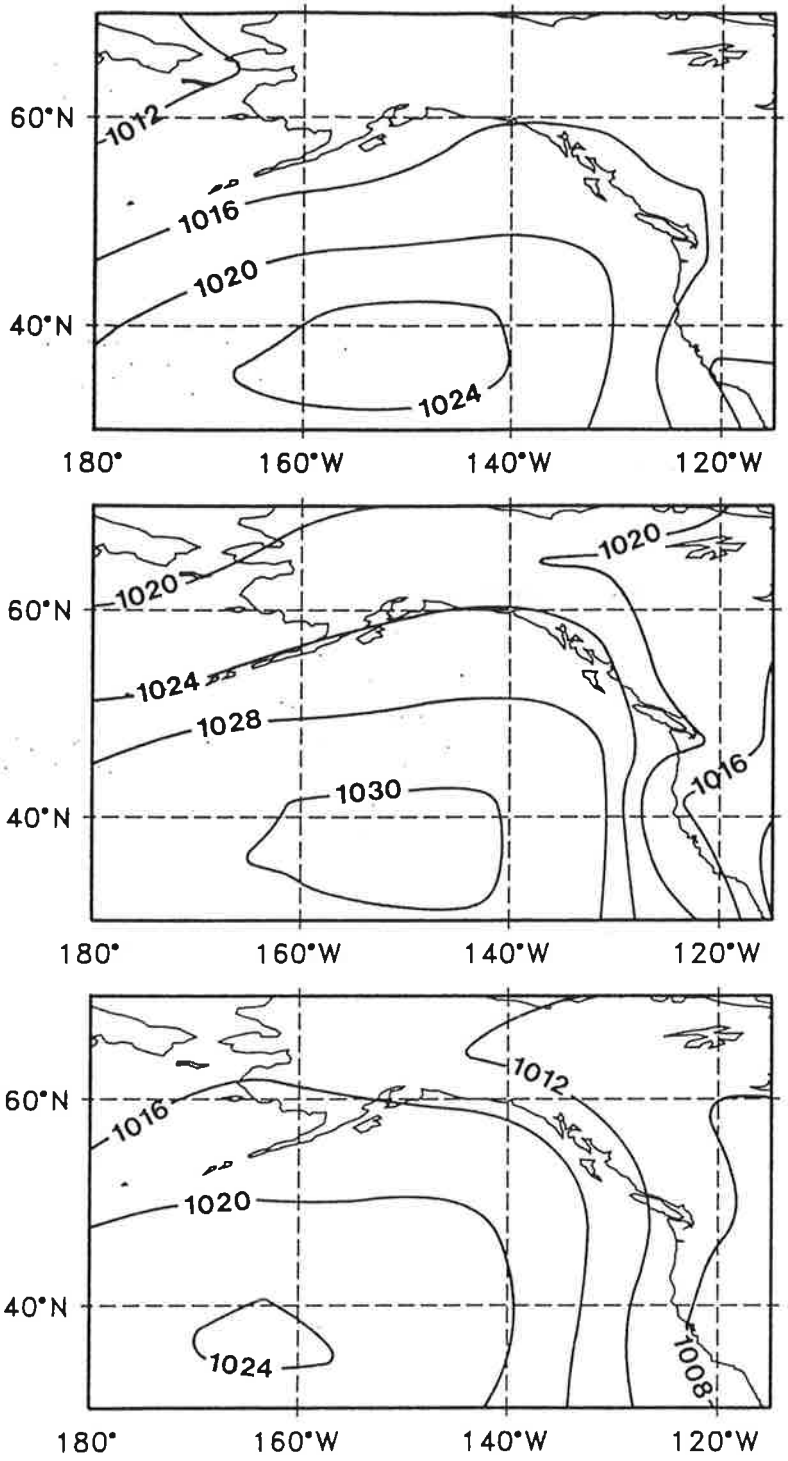

Figure 2 (cont.): July

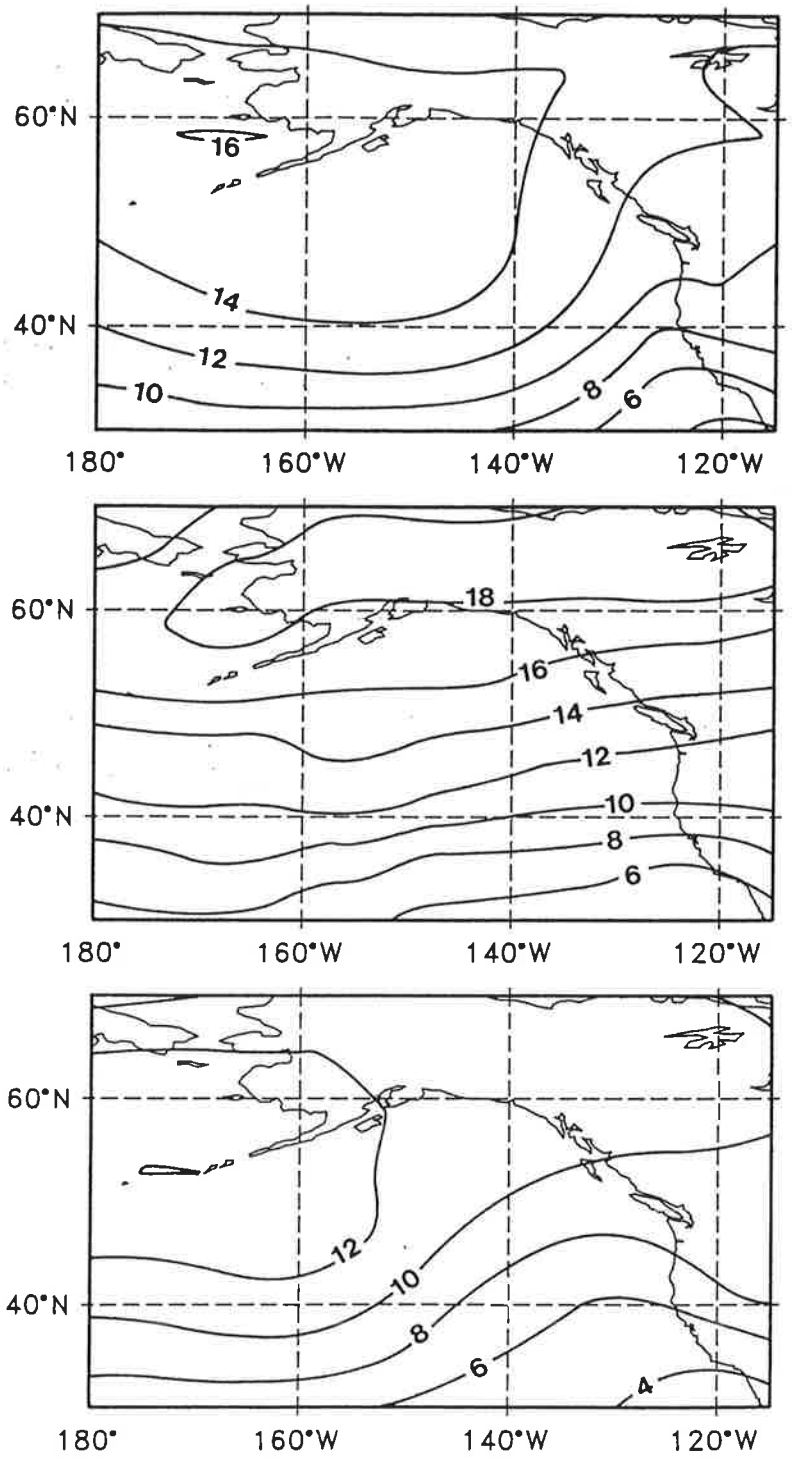

Figure 3. SLP standard deviation (mb) in the Pacific-North American sector as derived from the NMC analysis, the GFDL model and the MPI model: a) January;

4f

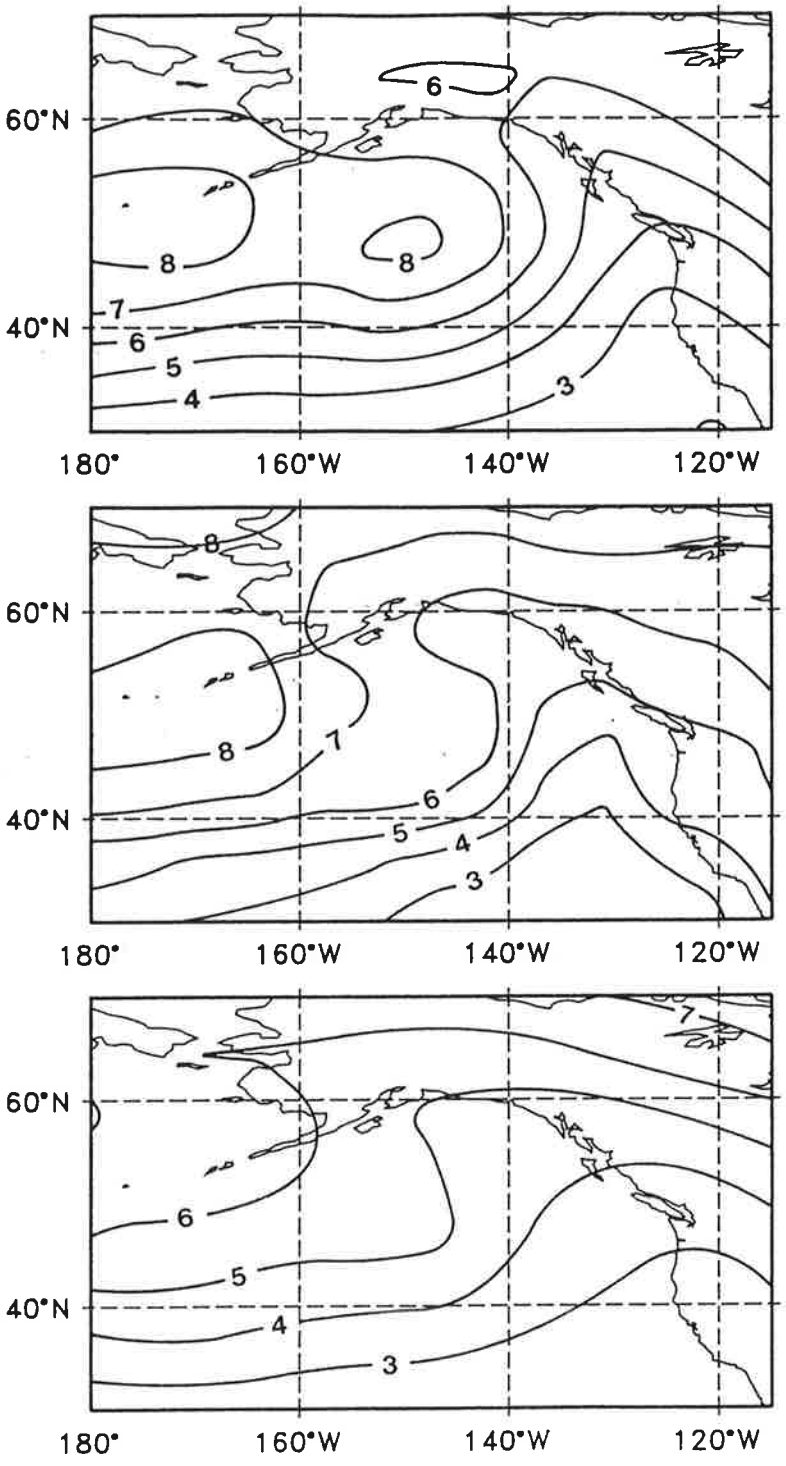

Figure 3 (cont): July

the MPI model is smaller than in the observations, and it also misses the variability maximum over the Pacific Ocean, whereas the GFDL model replicates quite well the variability distribution.

The coherent patterns of the SLP variability have been identified using EOF analysis, separately for the winter (DJF) and summer (JJA) months. Fig. 4 depicts the first four EOFs of the SLP anomaly field, along with their relative explained variances. In winter both models are able to reproduce the pattern of the first EOF, although the explained variance is underestimated by the MPI and overestimated by the GFDL model. Lower order EOFs are in general well-reproduced by the MPI run, whereas in the GFDL model the second and third EOFs are interchanged. In summer, the variance accounted or by the first EOF is again overestimated by the GFDL model and underestimated by the MPI model, which also produces a pattern that deviates from the observations. Other higher order EOFs are satisfactorily reproduced by both models.

A similar comparison between observations and the model simulations was carried out for the eastern American coast. For the observed mean SLP field in January (Fig. 5) the edge of the Icelandic Low can be seen, which is also present in the GFDL run with the right location and strength. In contrast, in the MPI simulation, this low is shifted too far southward. In July both models produce correctly the position of the quasi-permanent anticyclone over the North Atlantic, but in the GFDL run, its strength is overestimated, as was also the case for the North Pacific. With respect to the variability (Fig. 6) the NMC analysis for January shows a broad maximum of the SLP standard deviation over Greenland. In the MPI run this maximum is displaced somewhat to the southwest, whereas in the GFDL run this maximum is very distorted and elongated into the continent. In July, the observed SLP variability presents a marked zonal symmetry; this feature is also found in the MPI simulation, although the model tends to be more variable. However, in the GFDL run this symmetry is almost absent. With respect to the EOFs in the winter months (Fig. 7) the patterns simulated by the GFDL model do not resemble, even qualitatively, the ones derived from the historical data.The performance of the MPI model is much better in this respect. In contrast, in the summer, the GFDL model achieves much better results, most notably in replicating the first EOF, whereas the MPI results are not as good as in winter, especially for the lower order EOFs.

4. Weather State Classification

In this section, we describe an application of CART analysis to identify the weather states that are most closely related to the occurrence or absence of precipitation in four selected stations in the Columbia River basin of the northwestern US. Then, a stochastic model linking the weather states with the presence/absence of precipitation, and precipitation amounts, at selected stations was developed. In implementing this approach for the conditional simulation of station precipitation associated with GCM scenarios, two problems must be addressed. First, the long-term mean climate simulated by a GCM is usually biased with respect to the observations.This problem is usually avoided in sensitivity experiments with GCMs by considering only the differences between a control run and an anomaly run. This approach will be also followed here and in the CART classification scheme by performing the analysis using only anomalies of the SLP field. The CART procedure also requires for computational reasons that the number ofinput variables be limited, but at the same time, we are interested in capturing the essentials of the large-scale atmospheric circulation. For these reasons the input variables used in the CART procedure are the time series associated with the most important EOFs of the SLP anomaly field. To account for lags between thelarge-area pressure fields and local precipitation we used the EOF scores at the present and the previous day. In the Columbia River basin the stations selected for the CART analysis were Arrowrock Dam, Ellensburg, Stampede Pass and Wickiup. These stations provide a reasonable coverage of the basin and have a minimum of missing data in the period under study.

The results of the CART analysis for the winter months (DJF) are schematically shown in Fig. 8 and in Table 1. The CART procedure identified three weather states as defined by the binary decision

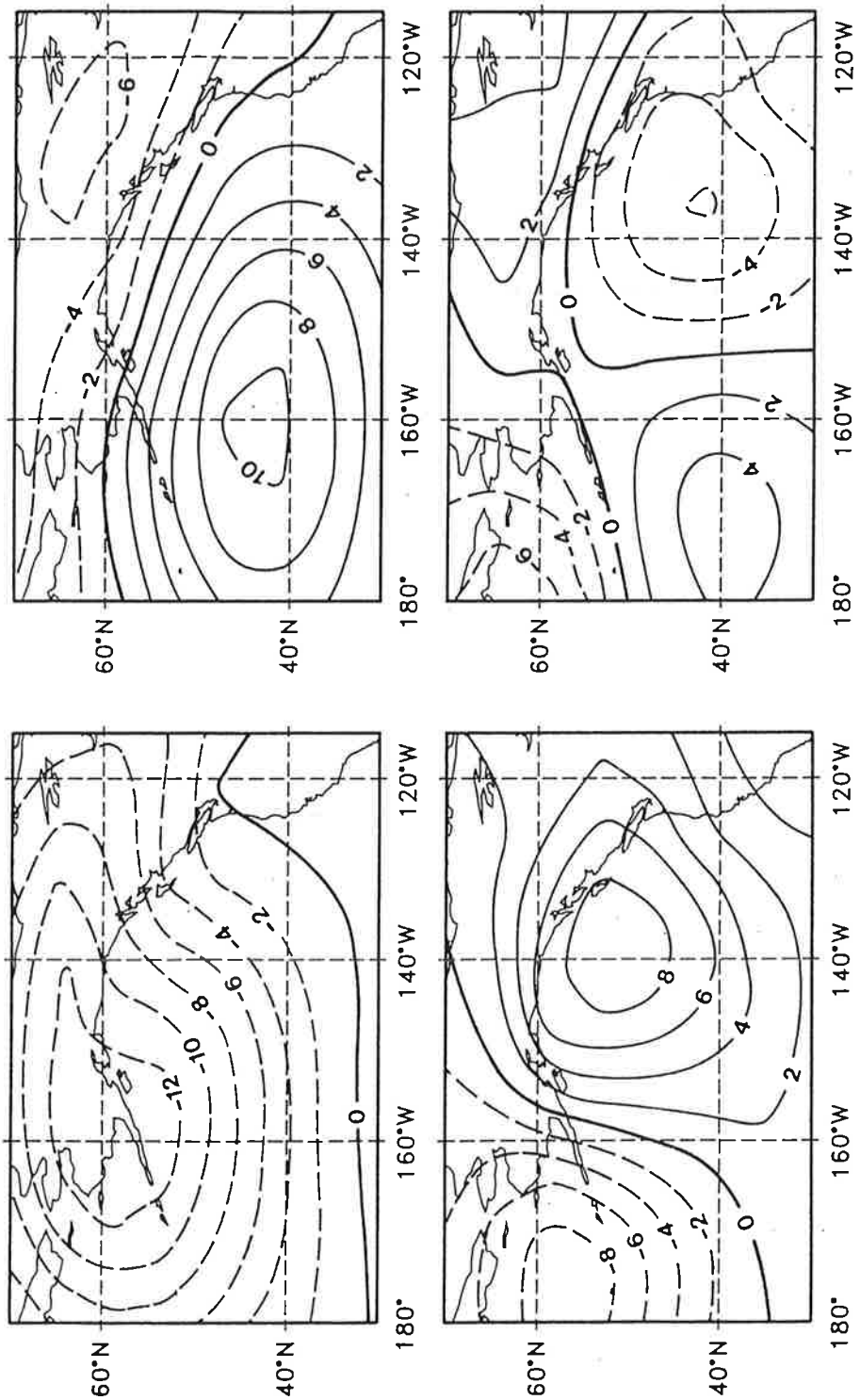

Figure 4. First four EOF of the SLP anomaly field (mb) in the Pacific-North American sector as derived from: a) NMC (DJF)

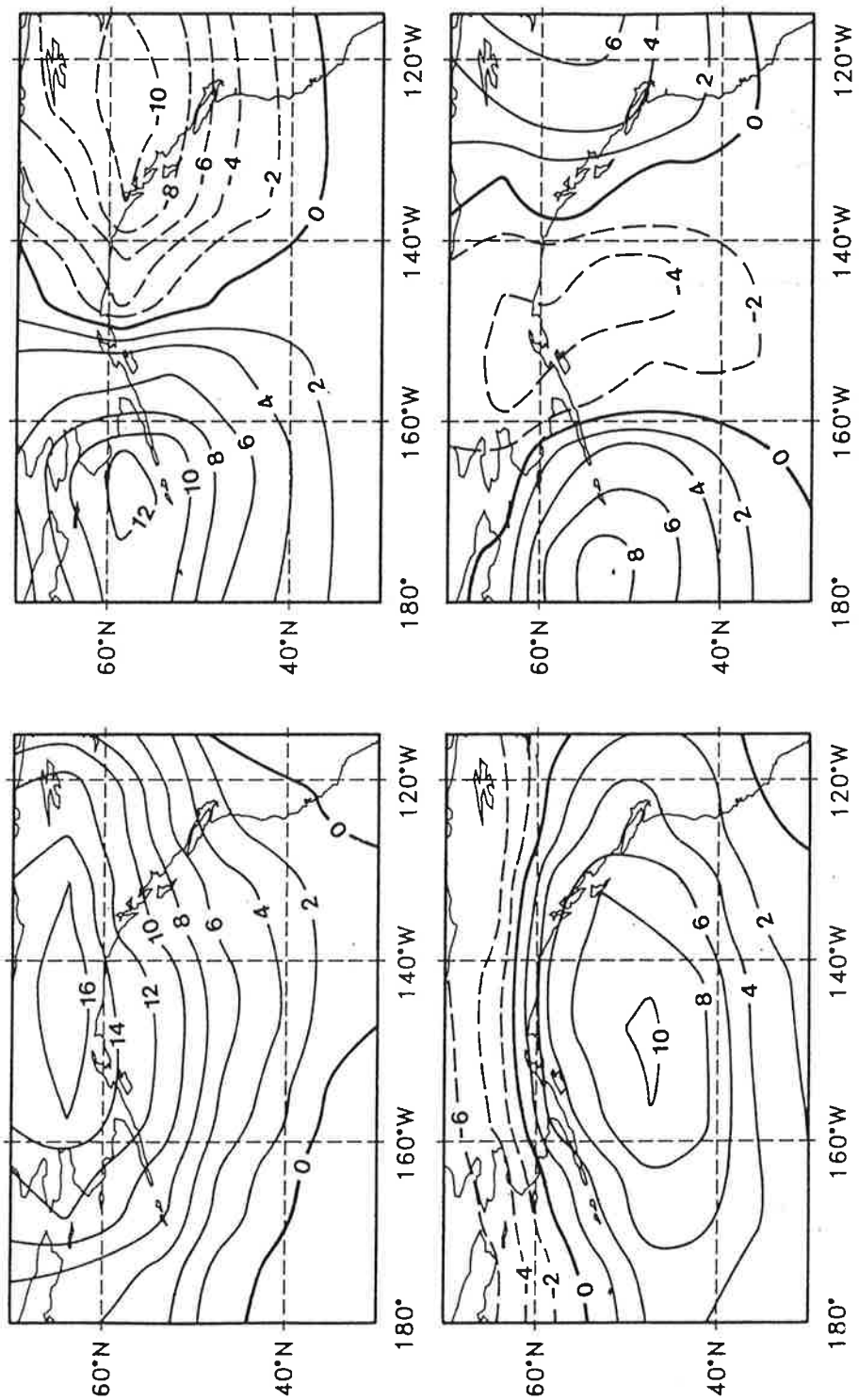

Figure 4 (cont): GFDL, (DJF)

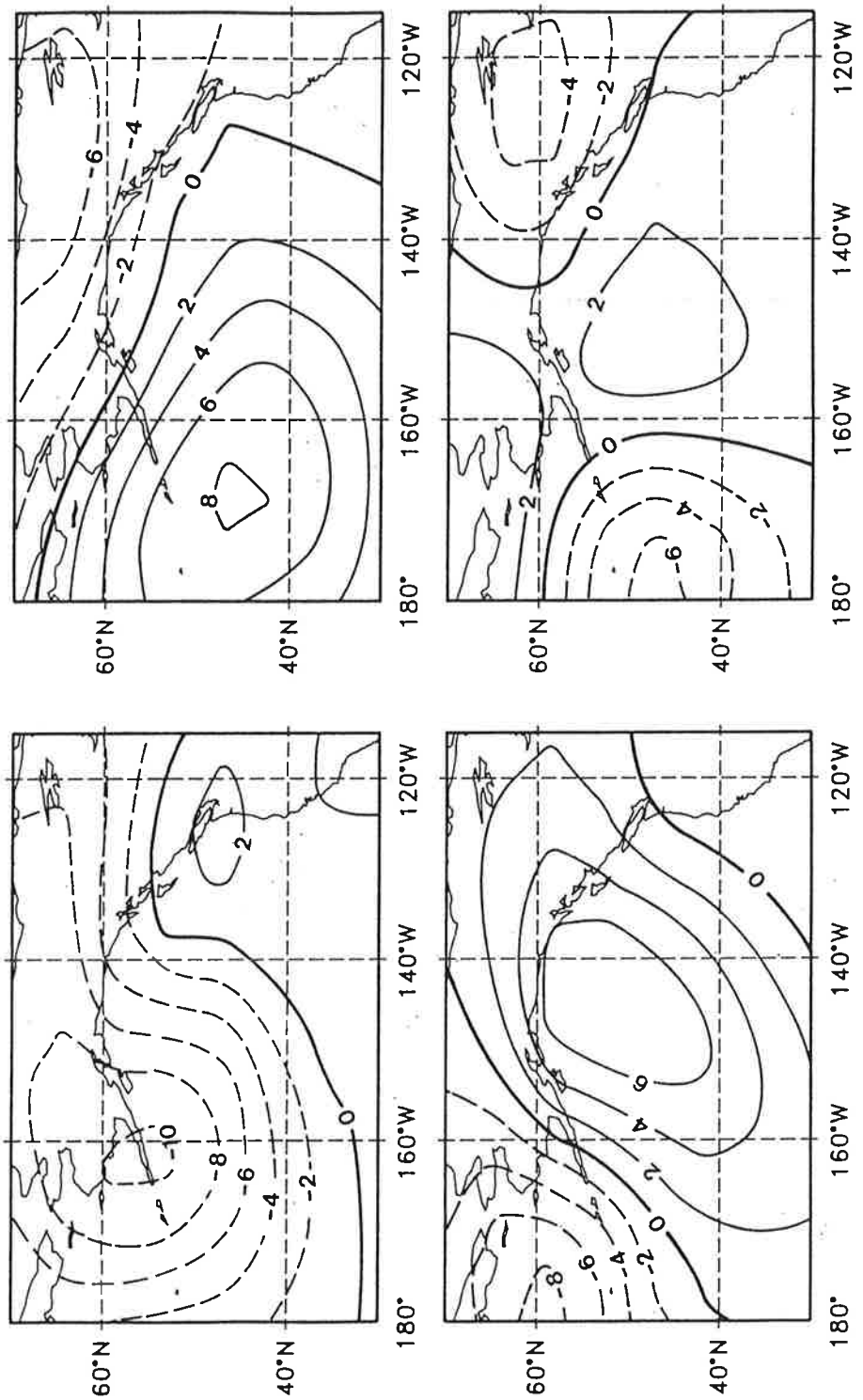

Figure 4 (cont): MPI, (DJF)

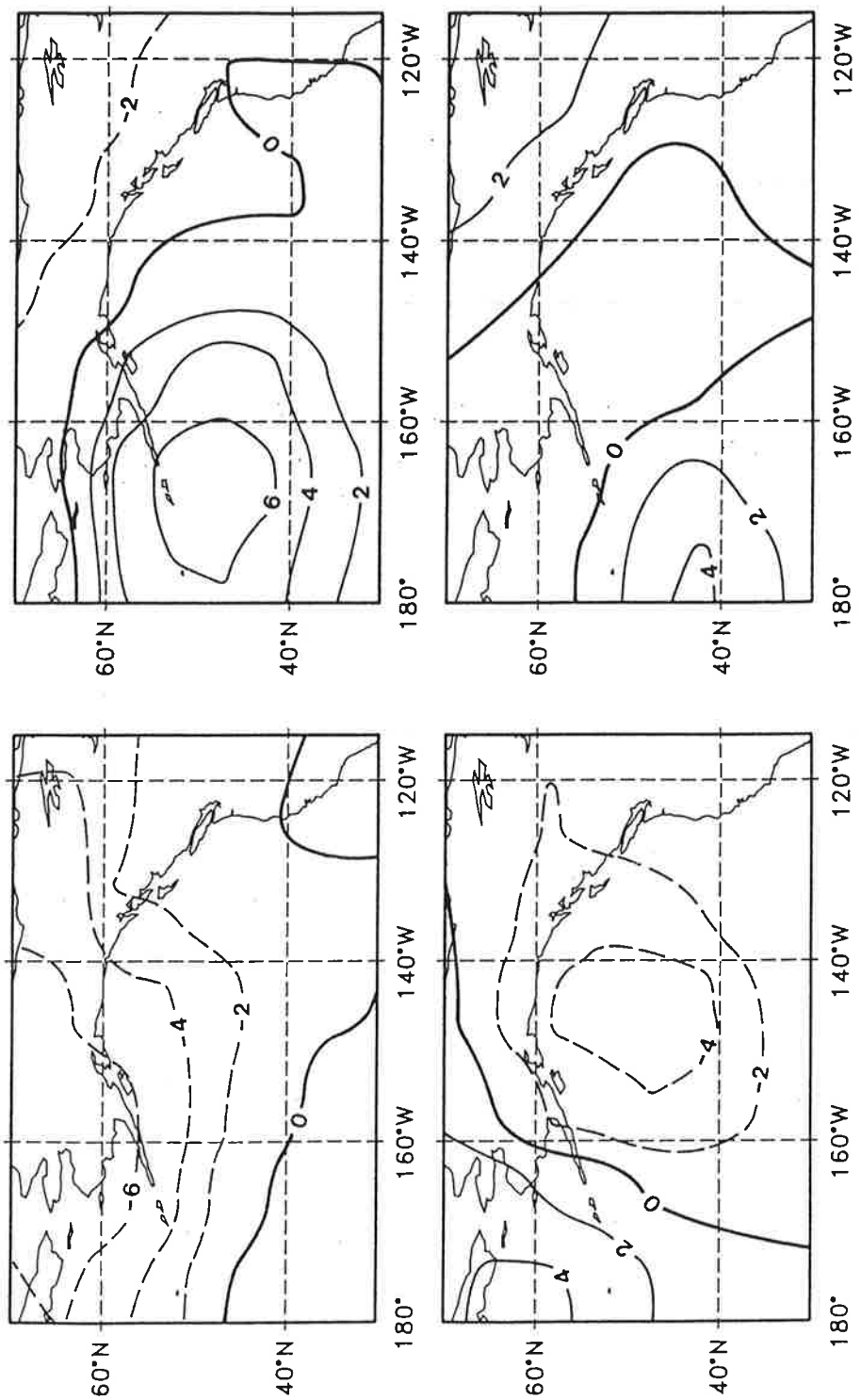

Figure 4 (cont): NMC, (JJA)

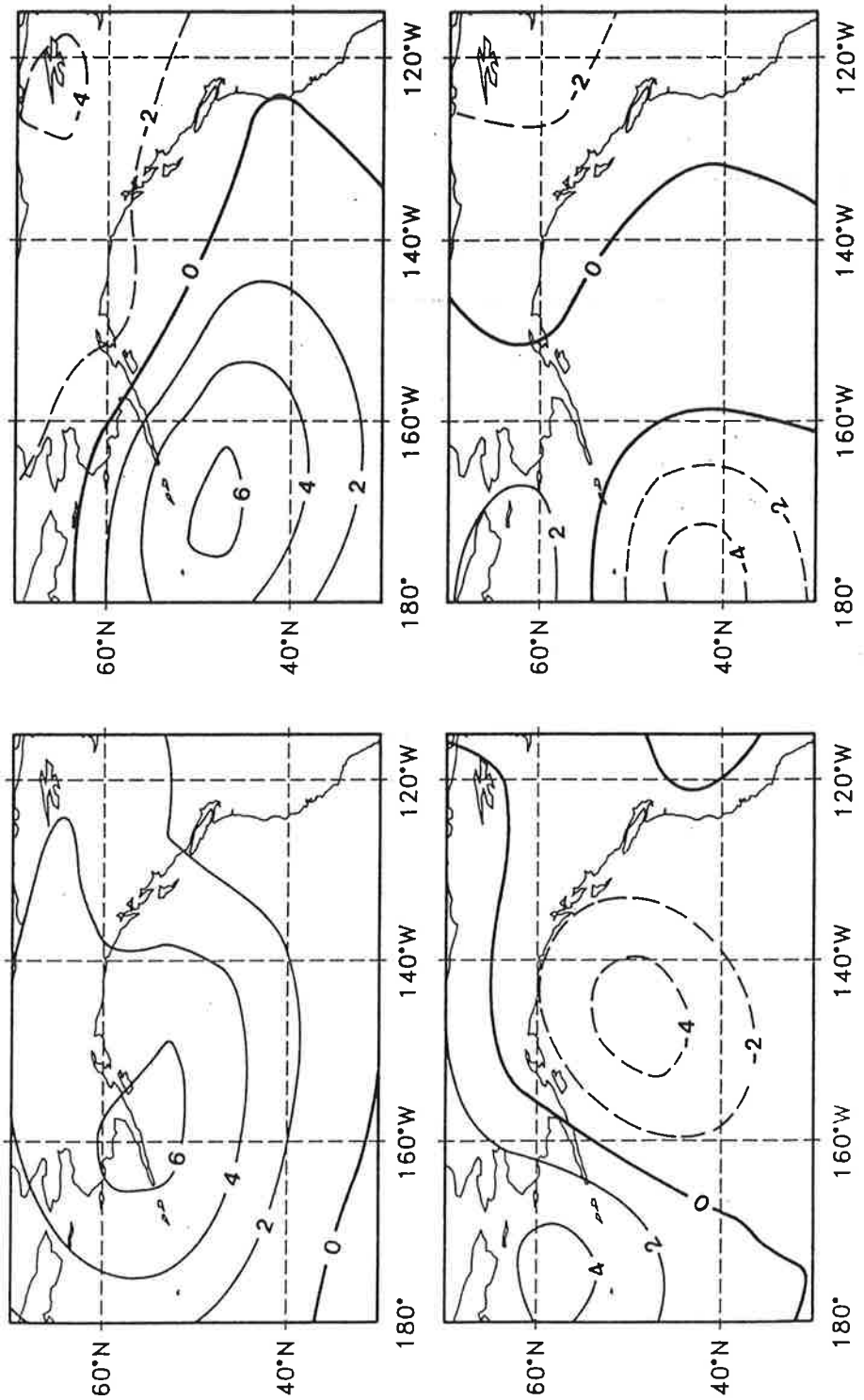

Figure 4 (cont): GFDL, (JJA)

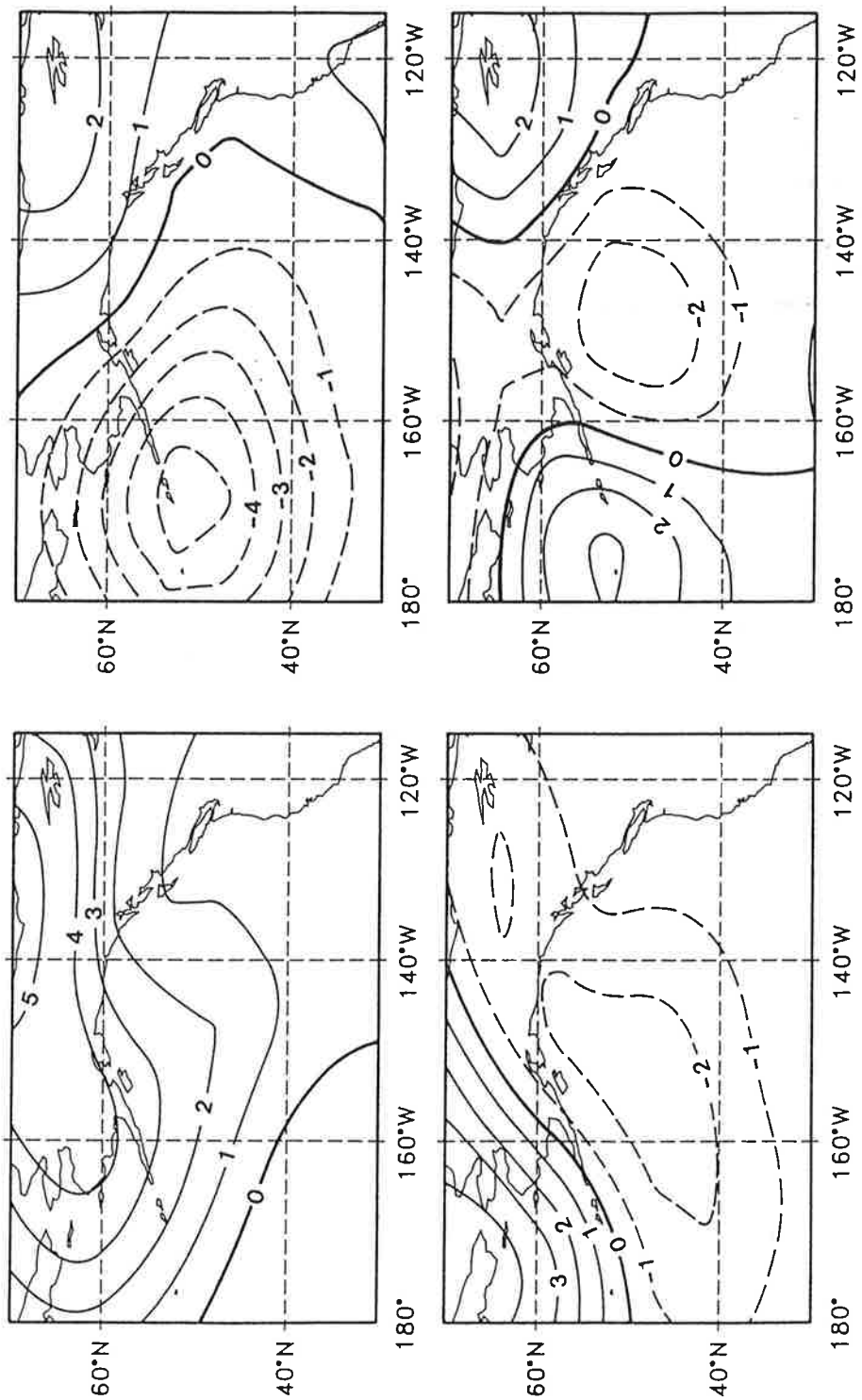

Figure 4 (cont): MPI, (JJA)

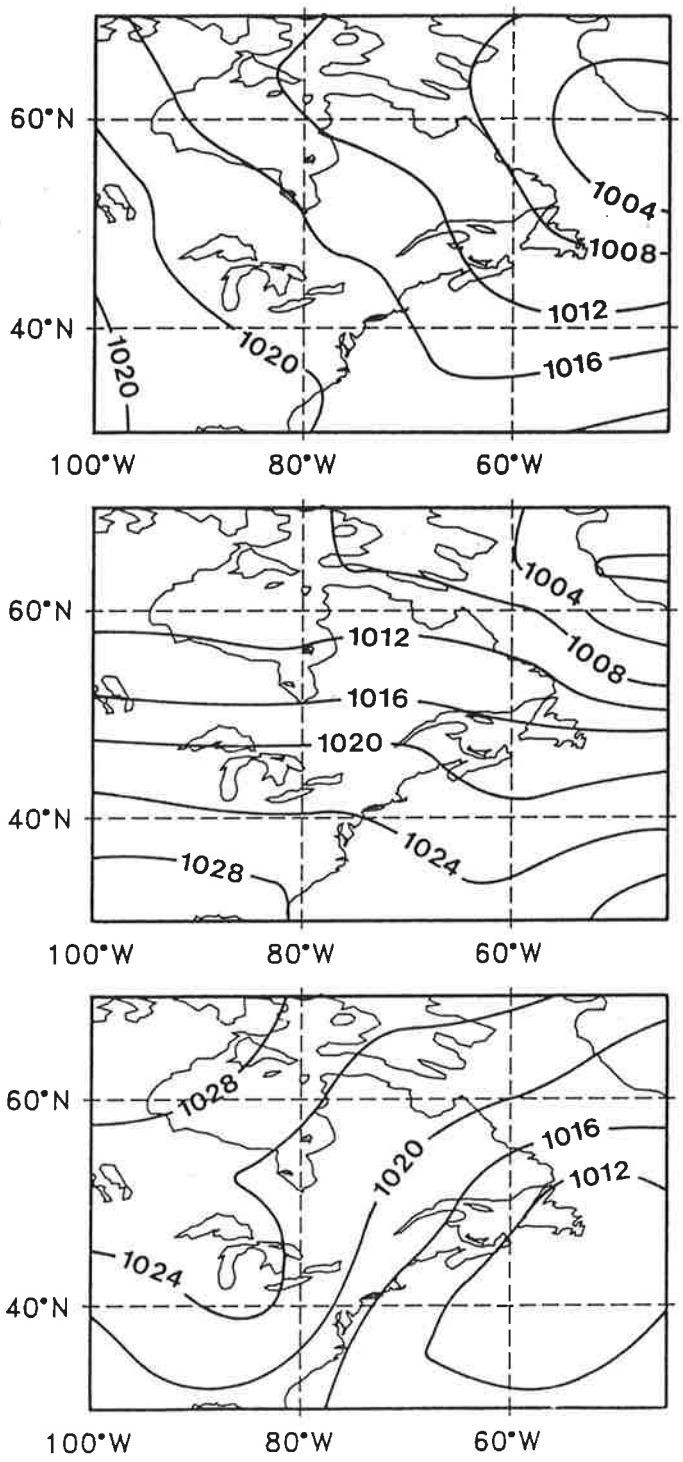

Figure 5. Mean SLP fields (mb) in the Atlantic-North American sector as derived from the NMC analysis, the GFDL model and the MPI model: a) January;

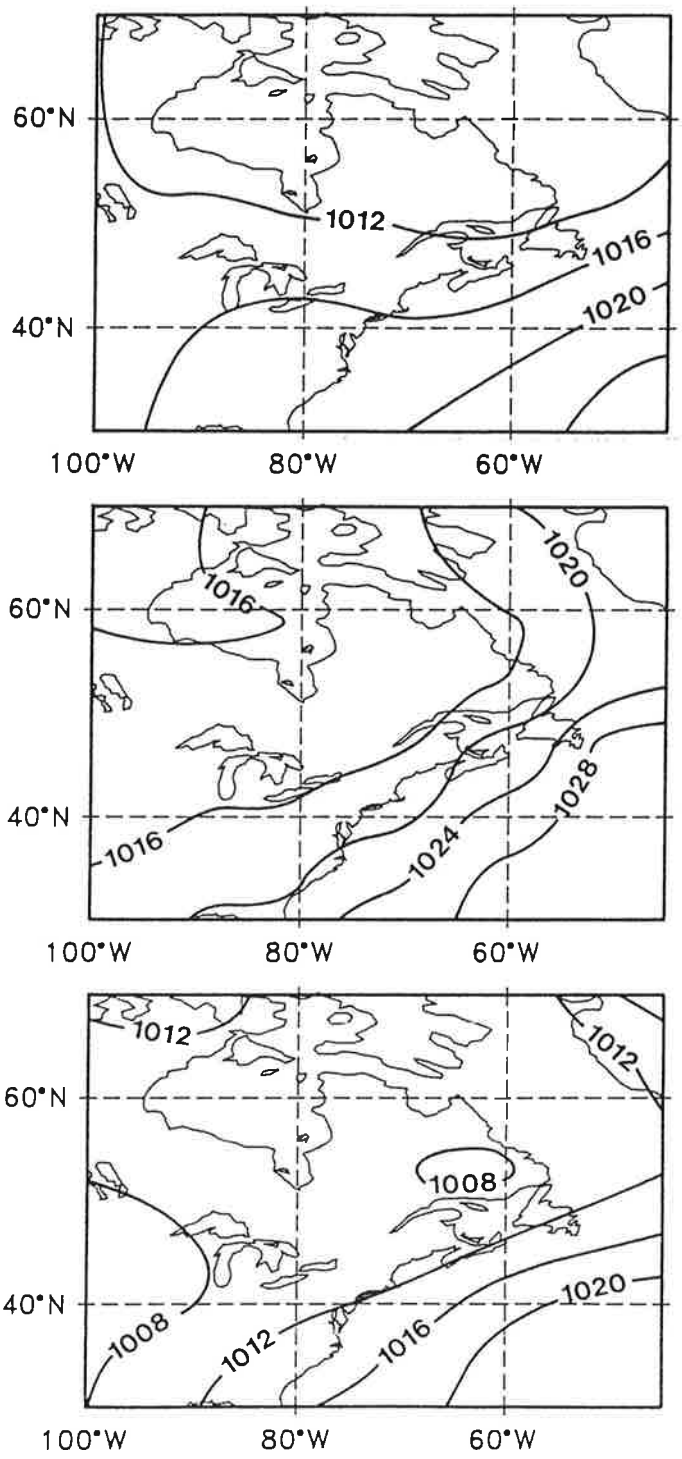

Figure 5 (cont): July

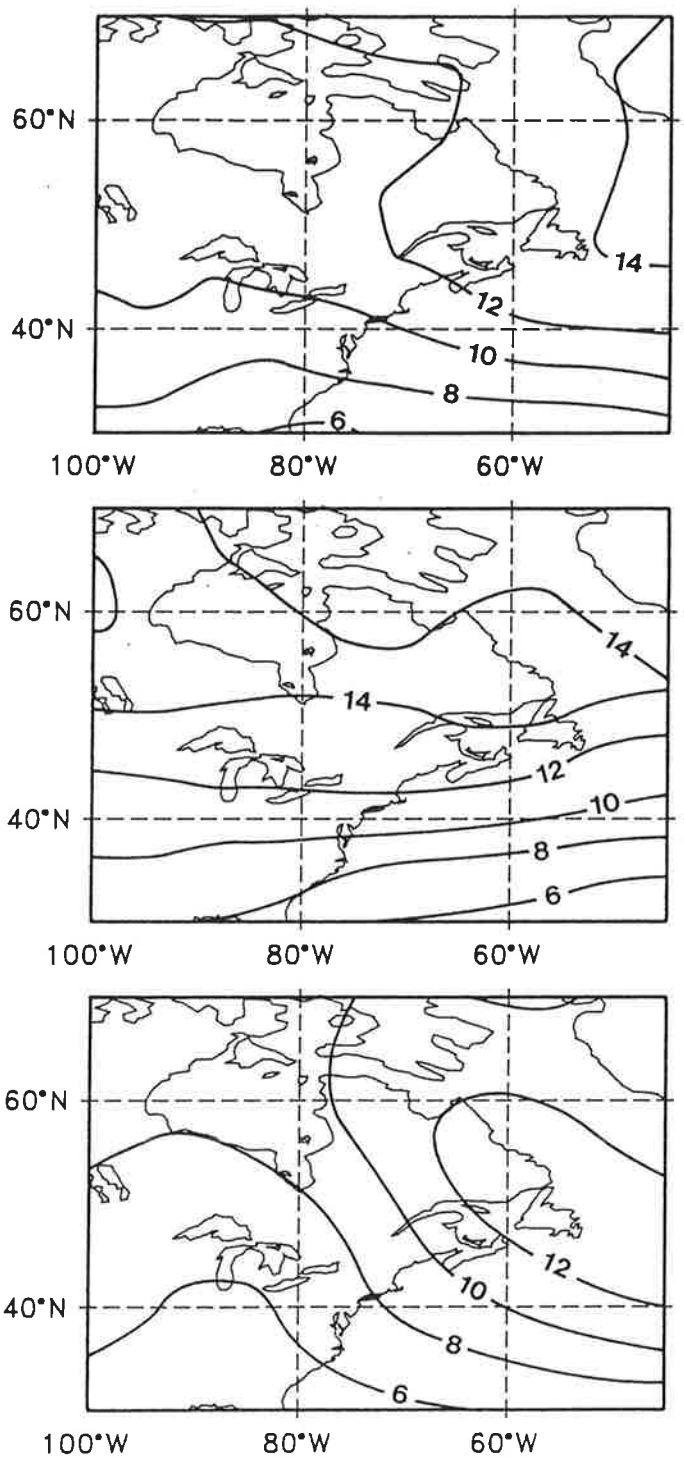

Figure 6. SLP standard deviation (mb) in the Atlantic-North American sector as derived from the NMC analysis, the GFDL model and the MPI model: a) January;

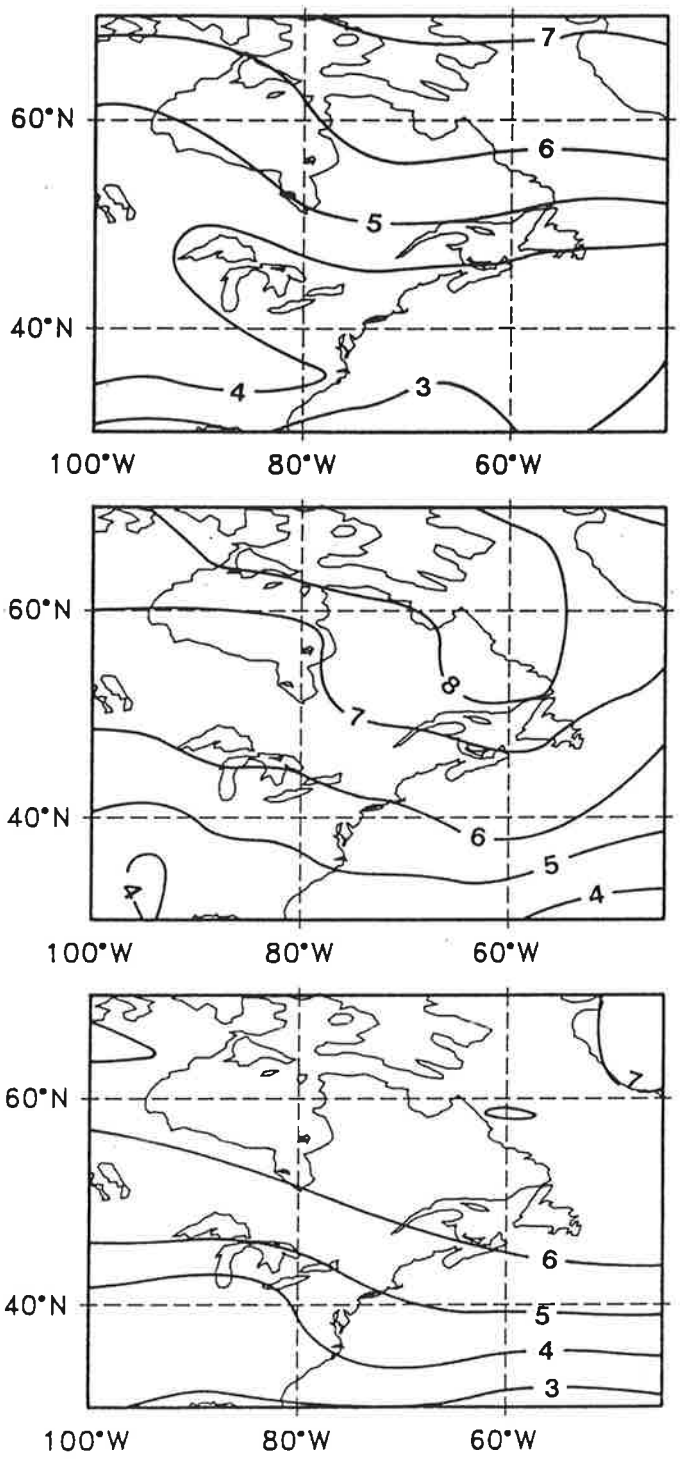

Fugure 6 (cont): July

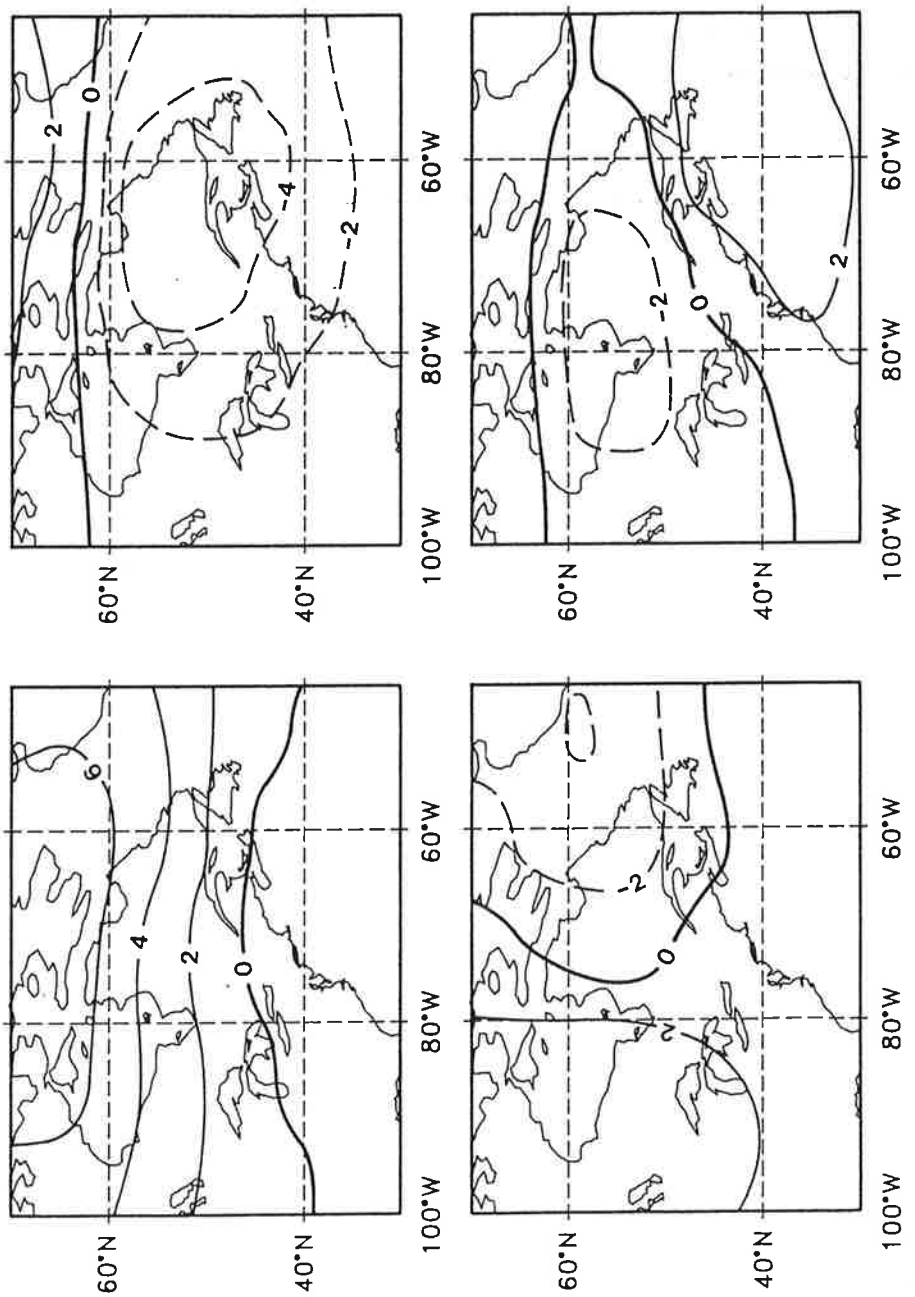

Figure 7. First four EOF of the SLP anomaly field (mb) in the Atlantic-North American sector as derived from: a) NMC (DJF);

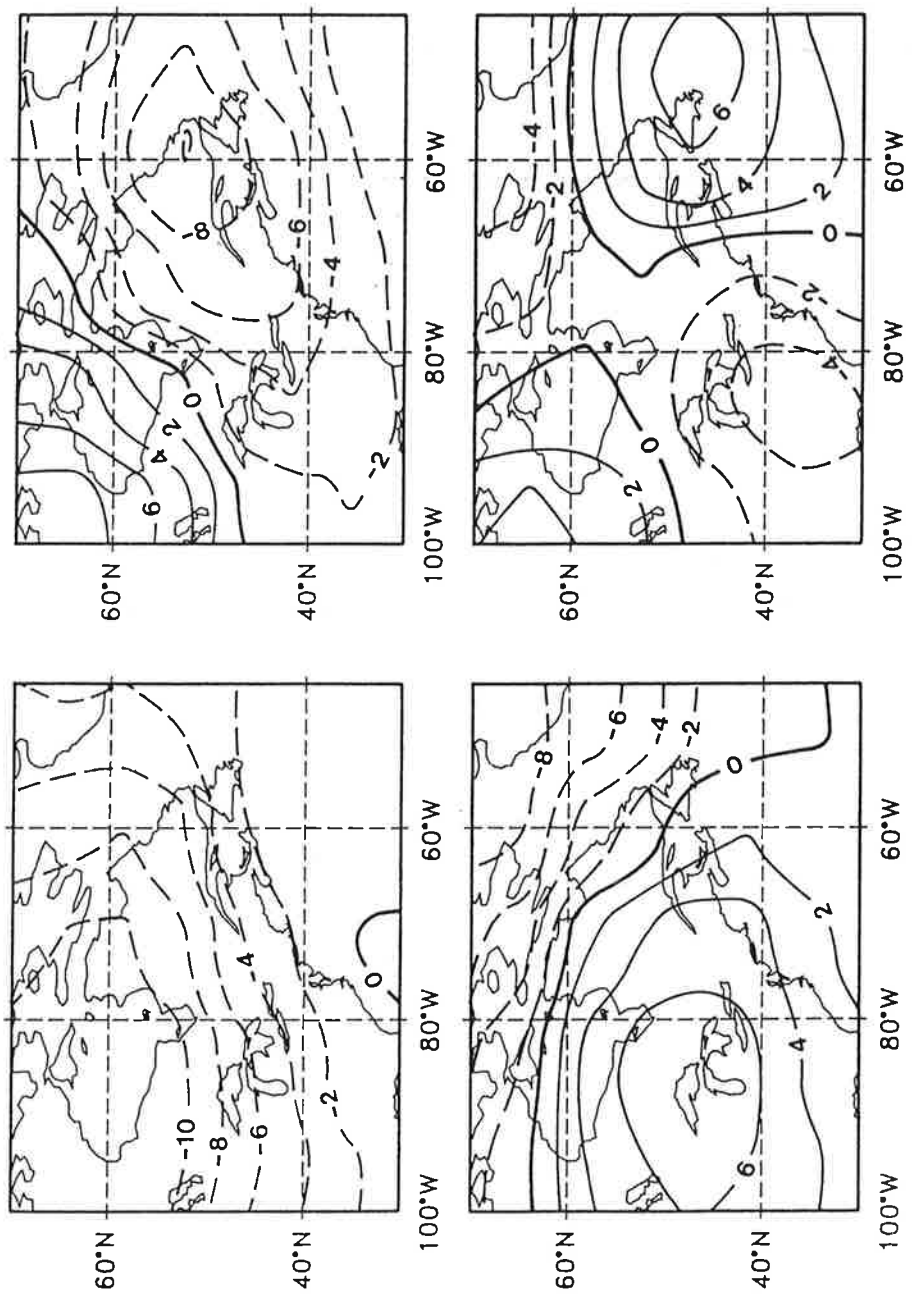

Figure 7 (cont): GFDL, (DJF)

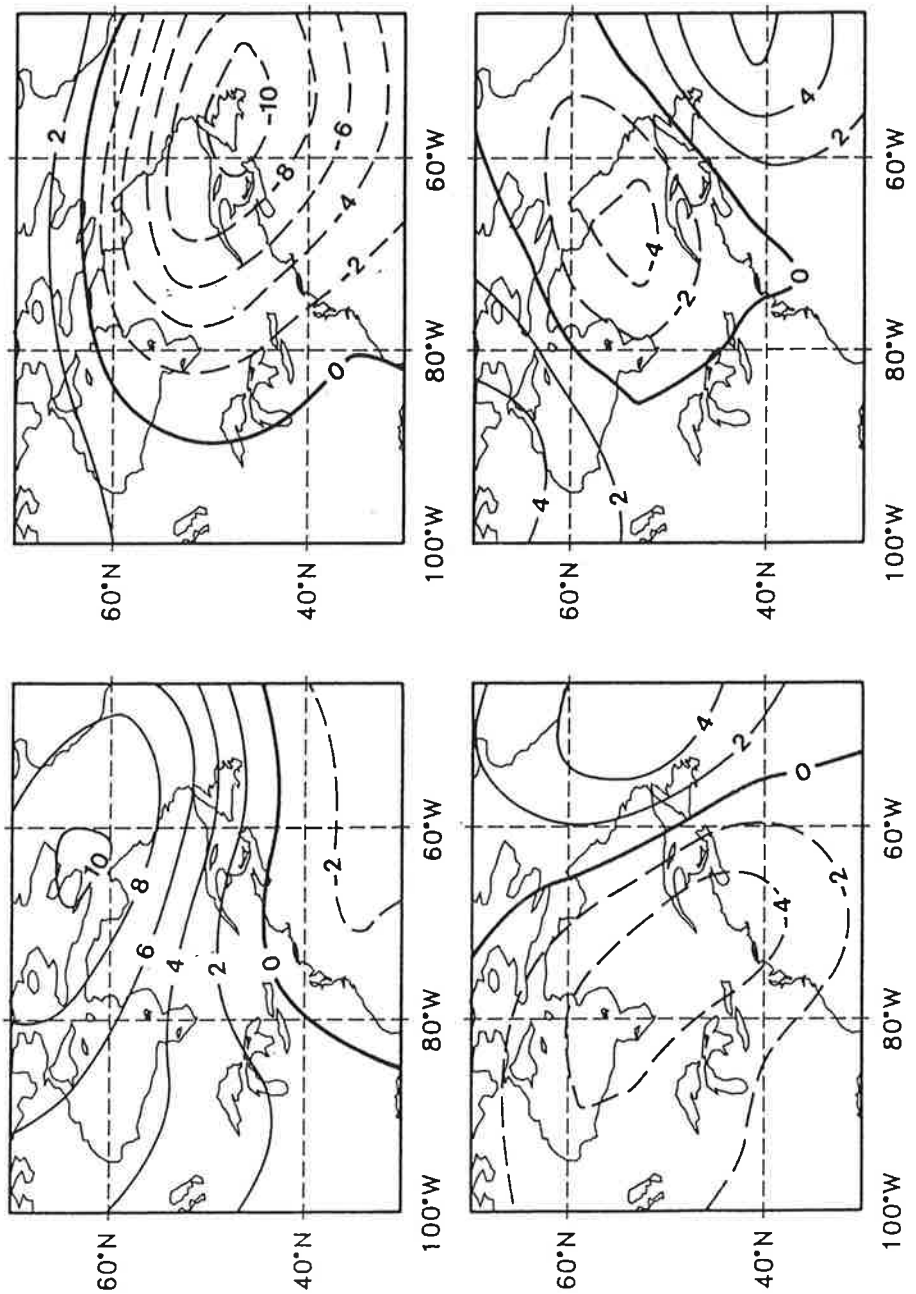

Figure 7 (cont): MPI, (DJF)

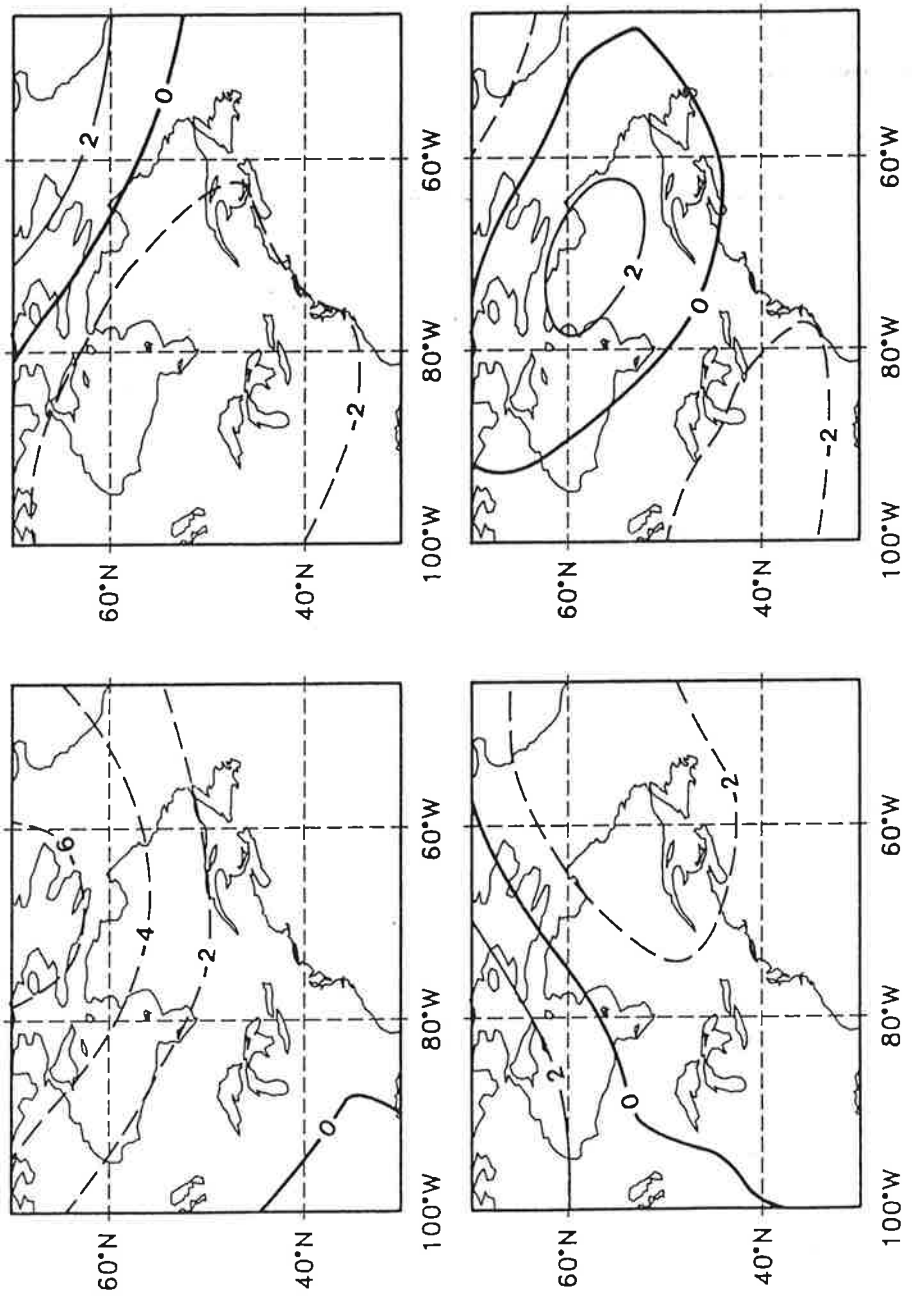

Figure 7 (cont): NMC, (JJA)

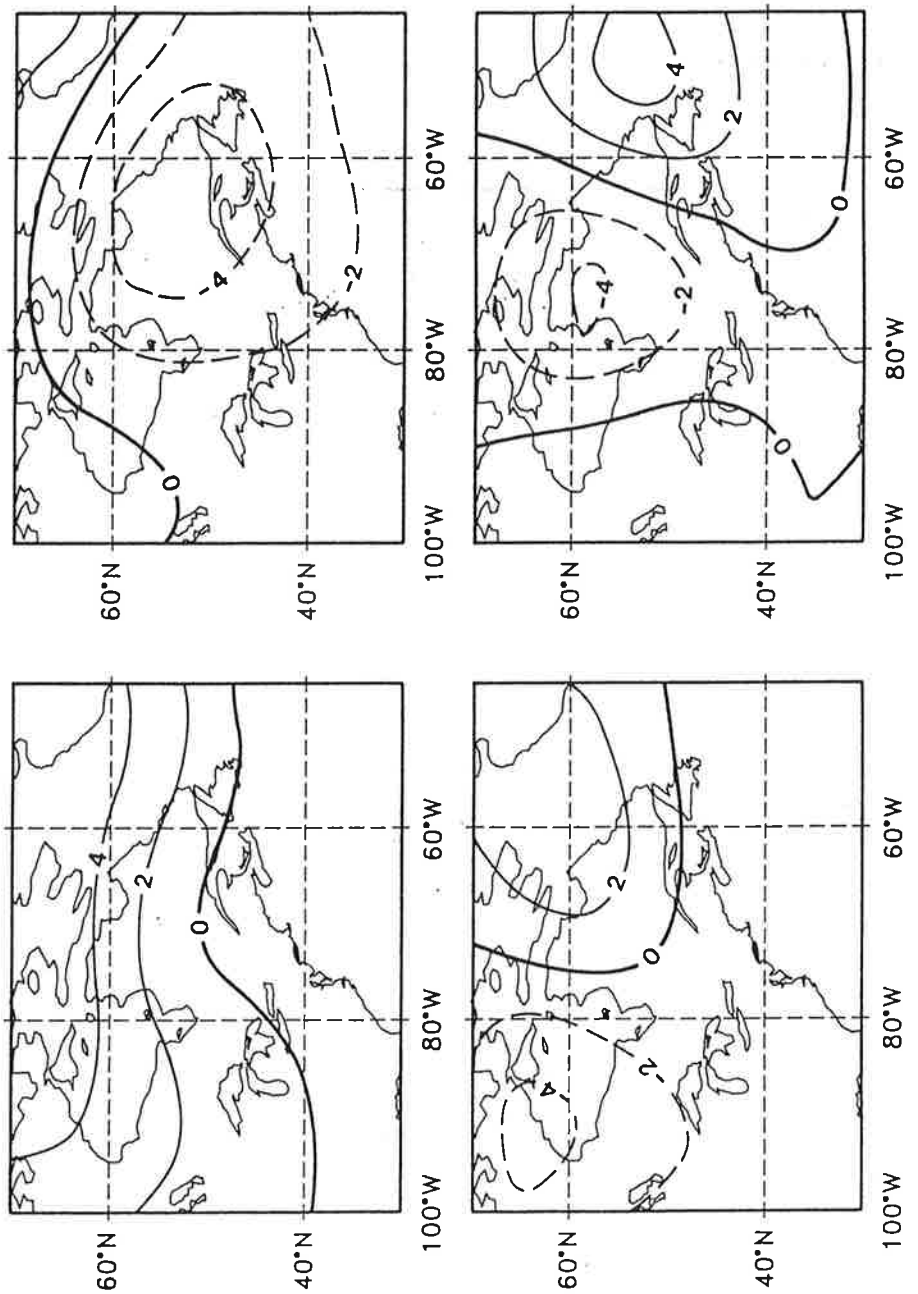

Figure 7 (cont): GFDL, (JJA)

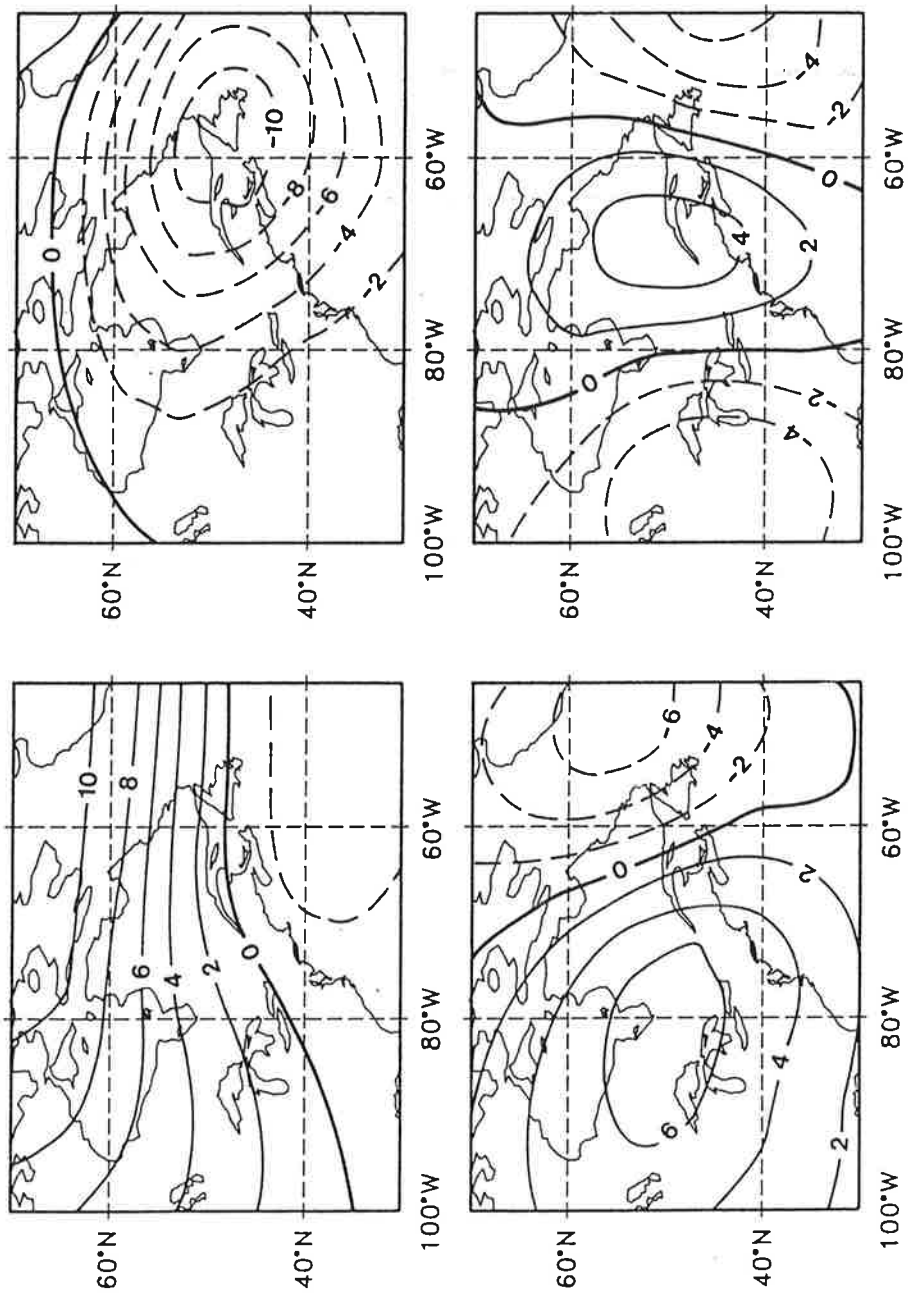

Figure 7 (cont): MPI, (JJA)

scheme illustrated in Fig. 8. The variables that are identified to define the weather states are the one-day-lagged scores of EOF 3 to discriminate between state 1 and the other two and EOF 5 to discriminate state 2 and 3. For instance, all days in which the score of PC 3 is less than -0.085 are classified as belonging to state 1. If not, they may belong to state 2 or 3 according to the value of PC 5.

Table 1. Most frequent rainfall patterns for each of the CART weather states n te Pacific-North American sector in DJF and their relative occurrence probability (conditional on the weather state).(A=Arrowrock Dam, E=Ellensburg, S=Stampede Pass, W=Wickiup; W=Wet, D=Dry).

Rainfall pattern A E S W	State 1	State 2	State 3
W W W W	.33	.06	.15
W W W D	.23	.11	.22
W W D D	.16	.09	.15
D D D D	.03	.39	.14

To illustrate the situations that give rise to each of the weather states, SLP composite plots based upon the days classified as belonging to each of the weather states are also displayed in Fig. 8. The most probable rainfall occurrence patterns at the four stations for each weather state can be found in Table 1. It can be seen that the first weather state is usually associated with the occurrence of precipitation at all stations. The third state is related mostly to no precipitation at any of the stations, whereas the second weather state may be accompanied by no rain, rain at the most western stations or rain at all of them. The interpretation of these results may be as follows: when the score of EOF 3 is negative (see Fig. 4) a lower-than-normal pressure cell sitting off the west coast of the U.S. advects humid air from the southwest into the continent. When the EOF 3 score is positive this mechanism does not operate but the CART procedure identifies another way by which rain may also reach some or all of the stations, as follows. EOF 5 (not shown in Fig 4) is associated with anomalous geostrophic zonal wind at approximately the latitude of the index stations. When the score of EOF 5 is positive the zonal (westward) circulation is enhanced and may bring some rain with it. Depending on the relative strength of EOF 5 and EOF 3 the rain may reach all stations, only the most western stations or none of them (state 2). If the EOF 5 score is negative both mechanisms work jointly to produce dry days at all the stations (state 3). The fact that the splitting variables are the one-day lagged scores should be roughly due to the time needed for the large-scale weather patterns over the Pacific to reach the stations in the continent.

A relevant question in this context is if the weather states identified by using data from these four stations are stable against changes in the number or location of the stations. A similar CART analysis was also performed retaining just two stations in the set: one located near the coast (either Ellensburg or Stampede Pass) and the other located in the interior (either Arrowrock Damm or Wickiup). It turned out that the weather states remained essentially the same. Furthermore the same weather states were identified when the data were split into two half-periods of ten years each. We also applied the CART analysis to individual stations in the Columbia River Basin. The discriminant variable between dry and wet states was always the score of EOF3, indicating that this statistical association is quite stable. We turn to this question again when presenting the results for the East Coast.

In the summer months (JJA) the CART procedure was not able to produce any decision tree when all fourstations were used, perhaps indicating that precipitation at each of the stations is not so closely related to one another in this season as it is in winter. This hypothesis was checked by removing the two interior stations (Arrowrock Dam and Wickiup) from the set and performing the CART analysis with the remaining two near-coast stations. In this case two weather states were found, defined by the classification scheme of Fig. 9 and Table 2. The precipitation occurrence distribution (Table 2) indicates that

Figure 8. Results of the CART analysis for the SLP field in the Pacific-American sector in DJF, derived from the NMC analysis and four stations in the Columbia River basin. The discriminant variables are PC3 and PC5. For instance all days in which PC3 is less than -0.085 belong to state 1. Plots correspond to the composite SLP fields calculated from the days belonging to each weather state. (See also Table 1).

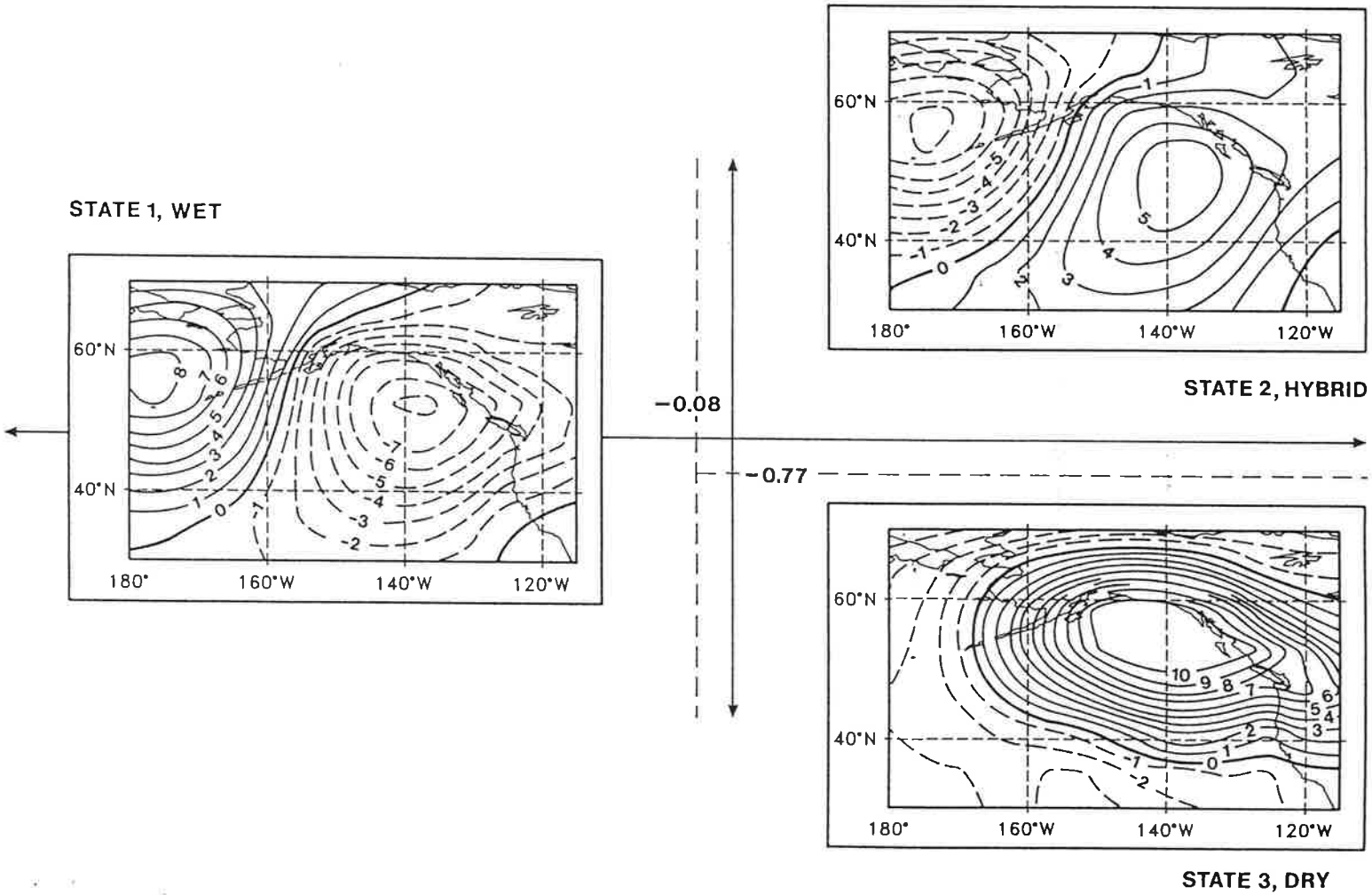

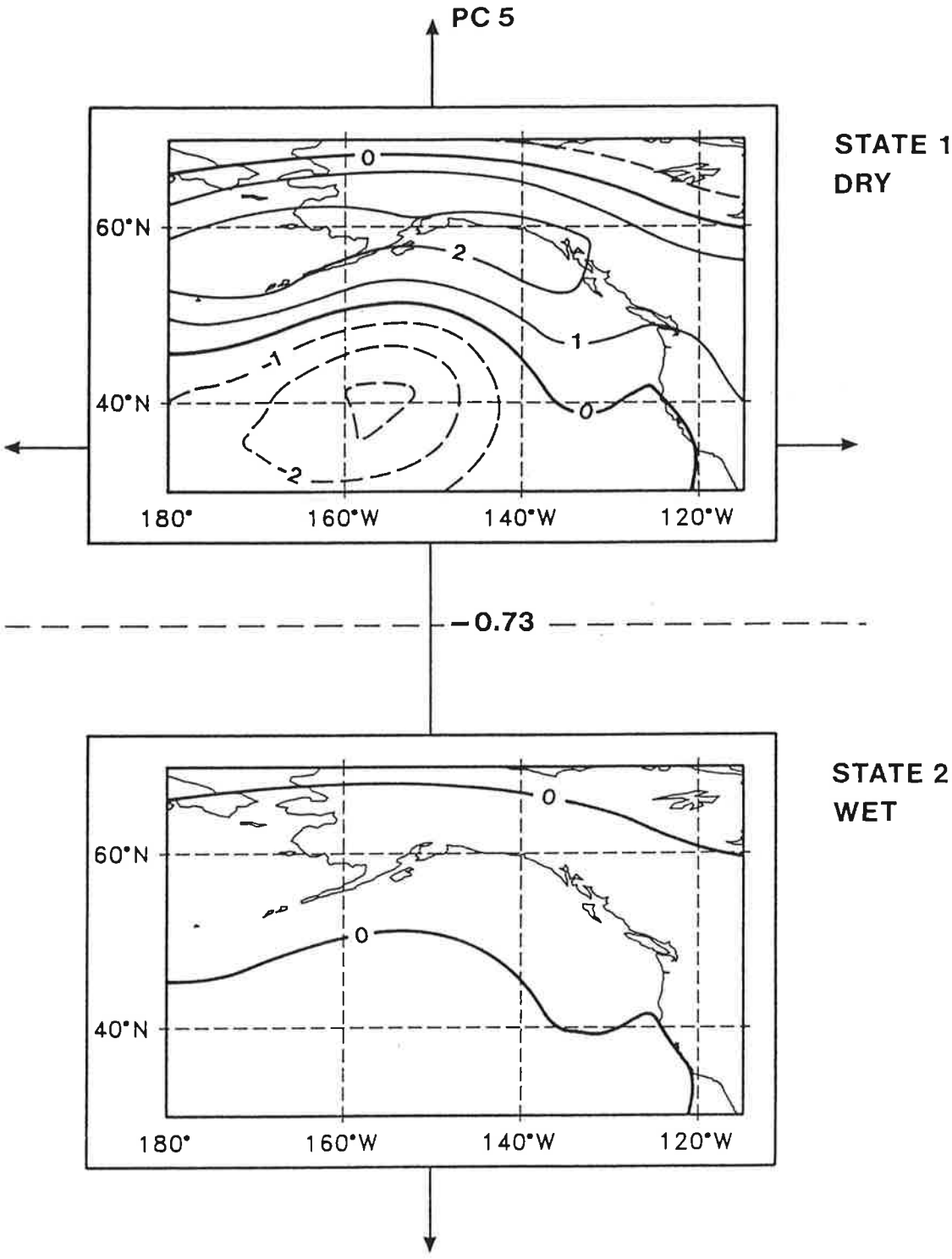

Figure 9. Results of the CART analysis for the SLP field in the Pacific-American sector in JJA, derived from the NMC analysis and four stations in the Columbia River basin. The discriminant variable is PC5. Plots correspond to the composite SLP fields calculated from the days belonging to each weather state. (See also Table 2).

these two states are mainly associated with dry or wet days in both stations simultaneously, respectively. The only node in the tree is split upon a relatively large (negative) value of PC5.

Table 2. Rainfall patterns for each of the CART weather states in the Pacific-North American sector in JJA and their relative occurrence probability (conditional on the weather state).(E=Ellensburg, S=Stampede Pass; W=Wet, D=Dry)

Rainfall pattern E S	State 1	State 2
WW	.21	.43
WD	.11	.11
DW	.10	.14
DD	.58	,32

Composites calculated from the days belonging to each states are also shown in Fig. 9, which can be interpreted using the same ideas as in winter: for days in which PC5 is negative a high-pressure zone is sitting northwest of the two stations, preventing moist air from reaching the coastal areas and giving rise to the dry state. The reverse reasoning is valid for the wet state. I f either of the interior stations is included in the analysis, the CART procedure is not able to find any classification of weather states. We believe that the reason is that summer precipitation is produced by processes of smaller scale than in winter. The classification of weather states for the East Coast of the US turned out to be more difficult. Initially a set of four stations was selected (Delaware, OH; Hatteras, NC; Hightstown, NJ; and Newport, TN) with a geographical separation roughly of the same order as those in the Columbia River basin. However, no classification tree could be created for these stations by the CART procedure, either in winter or in summer. We applied the CART analysis to three stations located closer to one another (Baltimore, MD; Hightstown, NJ; and Lexington, VA), again with negative results for both seasons. An attempt was also made to identify weather states by using a smaller region in the EOF calculation, with the hope of identifying smaller scale process that could be relevant for all the stations simultaneously,but this also proved to be unsuccessful. Only when two stations (Baltimore and Hightstown) situated fairly close to each other were used could a tree be created for the winter months, however even in this case no tree was found for the summer. CART analysis was also applied to individual stations. For some of them no classification scheme could be found, suggesting that the large-scale EOFs cannot discriminate between dry or wet days at these stations. For others, the discriminant variables were different for each station (except for Baltimore and Hightstown in winter), indicating that they are loosely related to each other. This is in contrast to the findings for the West Coast. It seems that the eastern U.S. winter precipitation is governed by smaller scale processes as compared to the West. For this reason no results of the CART analysis for the East Coast will be presented.

5. Weather States in the GCM simulations.

Once a relevant set of weather states has been identified it is interesting to investigate if these states can be realistically simulated in the GCM runs. One difficulty arises from the fact that the weather states are defined in terms of the EOFs derived from the observations, which may deviate from those derived from the GCM simulations. For instance, it has been noticed that the second and third EOF in the GFDL run in the West coast appear interchanged with respect to the observations. Therefore the scores cannot be directly used to classify the daily circulations into weather states. One consistent way to overcome this problem is to project the simulated SLP anomalies onto the same EOF patterns obtained from the historical data and use the resulting time series y (t) in the classification scheme:

$$y_j(t)=\Sigma\, f^i(t)\, g^i_j / \sigma^2_j \qquad (1)$$

where f^i (t) is the simulated SLP anomalies at time t and grid point i, g^i_j is the EOF j derived from the observations, and σ_j is the variance explained by EOF j. Since the area covered in this study is relatively small there is no need to account for the

shrinking grid-point separation with latitude. For the GFDL and MPI control runs the anomalies were calculated by subtracting therespective long-term mean from the simulated data, and therefore the possible bias of the models is removed. For the $2xCO_2$ MPI experiment, however, the long-term mean of the control run was used to retain the possible climate signal due to CO_2 doubling. The following weather state analysis can be used to validate the GCM's ability to simulate the behavior of observed regional synoptic situations. Our attention will be focused in two aspects: the probability of occurrence of each of the weather states and the log-survivor function of each state. This function is defined as

$$L(t)=\ln(1-F(t)) \qquad (2)$$

where F(t) is the cumulative distribution function of the state lifetime. Thus, the log-survivor function gives the probability that a certain state will last for at least t consecutive days. Tables 3 and 4 give the probability of occurrence of each state derived from the observations and from the three model runs in winter and summer,respectively.

Table 3. Probabilities of occurrence of the three weather states identified by CART analysis in the Western American Coast in DJF as observed and in the different model runs.

	State 1	State 2	State 3
Obser.	.46	.42	.12
MPI	.45	.48	.07
MPI ($2xCO_2$)	.44	.45	.11
GFDL	.52	.35	.12

Table 4. Probabilities of occurrence of the two weather states identified by CART analysis in the Western American Coast in JJA.

	State 1	State 2
Obs	.24	.76
MPI	.19	.81
MPI ($2xCO_2$)	.22	.78
GFDL	.24	.76

The differences between these parameters are in general small. This result is to some extent due to fact that the scores have by construction zero mean (by taking anomalies the model bias has been removed), so that when a node in the decision tree is split upon a very small (absolute) value of one variable it is likely that half of the days will be classified following one branch and the other half following the other one, regardless of the data origin. However this will not be in general the case if the node is split upon a non-zero value of a variable, since the standard deviations of the scores are in general different in the models than in the observations.

Fig. 10 depicts the log-survivor functions for the weather states derived from the NMC analyses and both GCMs. These functions are nearly straight lines, which should be the case if the transitions between states follow a purely Markov process. In that case the absolute value of the derivative would be the inverse of the exponential parameter τ. For the West in winter the GFDL model tends to produce longer series of state 1 (wet state) and state 2 (hybrid) and shorter series of state 3 (dry state) than were observed. The MPI model simulates correctly the lifetime of state 1 but underestimates that of state 2 and overestimates the life time of state 3. The doubling of atmospheric CO_2 causes a slight increase of the lifetimes of all the weather states in the MPI model. A plausible explanation might lie in an increased atmospheric stability due to a reduced meridional temperature gradient in the $2xCO_2$ climate. In summer, both models replicate properly the behavior of the dry weather state, whereas the GFDL generates shorter, and the MPI model longer, series of the wet state.

6. Precipitation generation for GCM experiments.

The weather state classification scheme can be used for the stochastic generation of precipitation

Figure 10. Log-survivor functions of the CART weather states in the Pacific-North American sector for the NMC analysis and in the different model runs:a) Winter; —— NMC; ---- GFDL; .... MPI; —— MPI ($2xCO_2$)

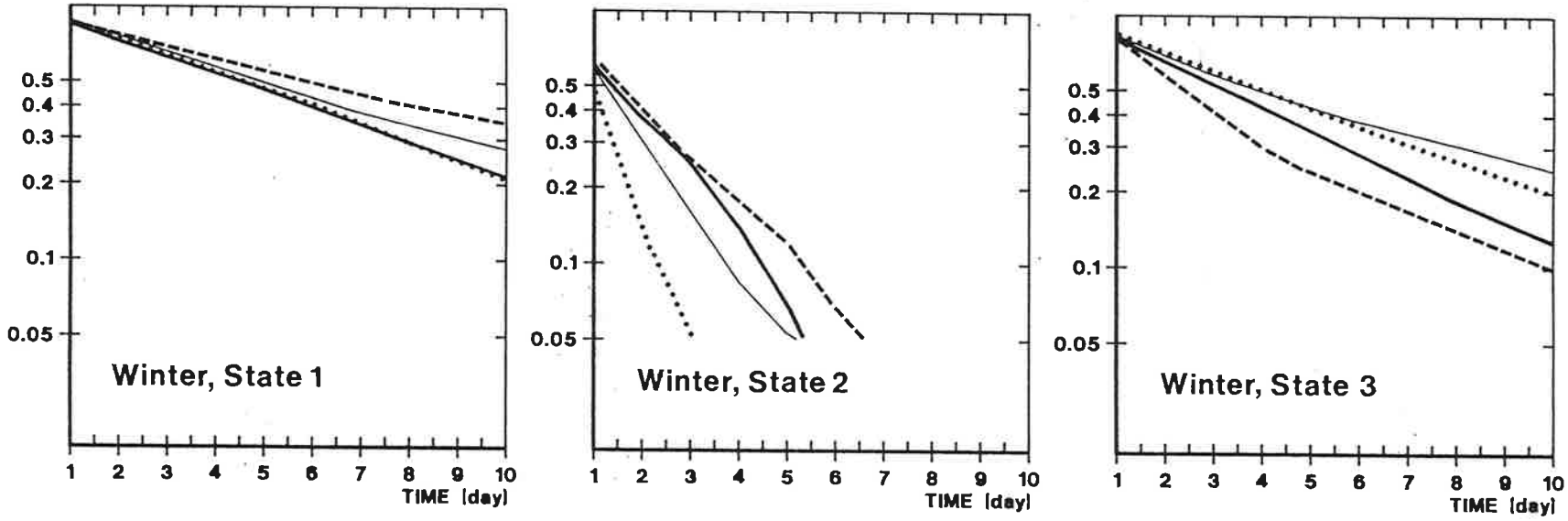

033EDZc

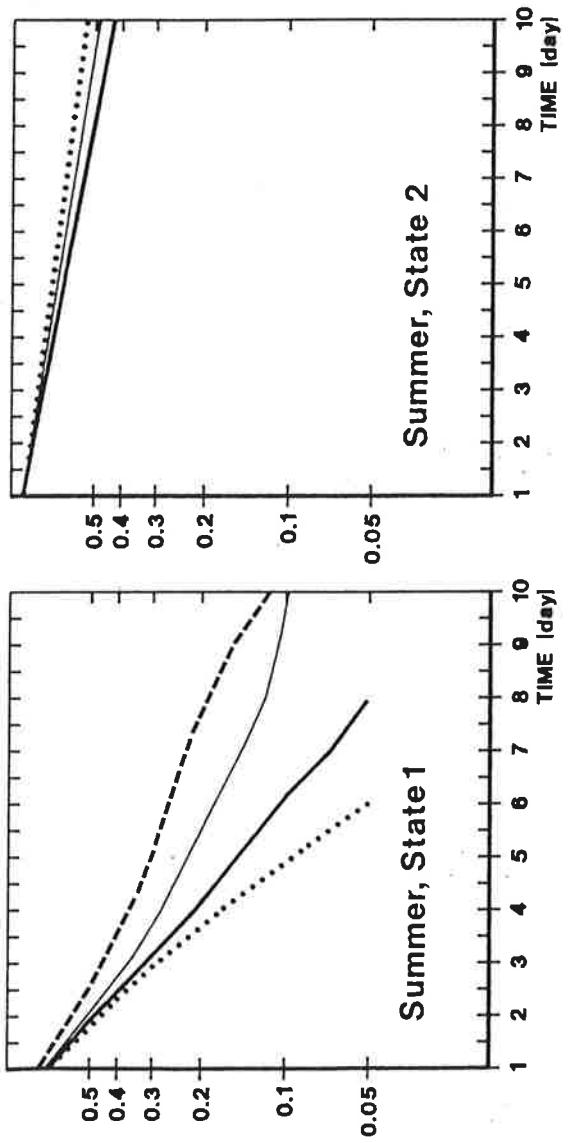

Figure 10 (cont): Summer; —— NMC; ---- GFDL; .... MPI; —— MPI ($2xCO_2$)

time series based on the daily circulations simulated by the GCMs. Since the present generation of GCMs lack the necessary resolution to simulate precipitation reliably at specific stations, the precipitation generator is an alternative method to transfer the results of the GCM experiments to the local scale.

In this section two different stochastic precipitation generators aredescribed. The first is based on the CART classification scheme. Although in general this method behaves satisfactorily, the precipitation generator based on CART proved to be unsuccessful in replicating some aspects of the precipitation processes, such as the storm interarrival times. This quantity is fairly important when precipitation time series are used by hydrologists to drive catchment (precipitation-runoff) models. Therefore, a second type of precipitation generator, based on a modified analog method, was also explored in an attempt to resolve some of these deficiencies.

6.1 *Precipitation Generator Based on CART*

The first method for generating precipitation sequences is based on the CART classification scheme. This method consists of applying the CART tree to each day of the historical record, which is assigned the value of the resulting weather class. The precipitation values for each day of the historical record are then assigned to "bins" associated with each of the corresponding weather states. Given a sequence of weather states (for instance, resulting from the application of CART to a GCM simulation run) the simulated sequence of precipitation states is determined by sampling, with replacement, from the appropriate bin.

This procedure was applied to the three GCM experiments (GFDL and MPI base climate, and MPI $2xCO_2$. Initially, though,the performance of this method was checked by analyzing the results produced when the input weather classes were taken from the observation series (NMC data); the resulting conditional simulation of precipitation was then compared with the precipitation that actually occurred (in the sense of precipitation presence/absence). Because the procedure is not restricted to generating precipitation for the stations used to "train" the CART algorithm (Arrowrock Dam, Ellensburg, Stampede Pass and Wickiup), we illustrate the simulated results for an independent station, Forks (located along the Pacific Coast). We will focus on three properties of the simulated precipitation that are of concern to hydrologic modelers: mean precipitation, storm interarrival times, and the daily precipitation probability distribution. It should be noted that, because the precipitation is resampled from the historical record, there is no point in comparing simulated and observed quantities such as the absolute maximum of daily precipitation or spatial precipitation correlation: these quantities are essentially the same in the simulated and observed records.

The precipitation time series generated from the GCM simulations cannot, of course, be compared directly with the observations; the comparison must, of necessity, be with the long-term mean precipitation (Table 5).

Table 5. Mean rainfall (mm/day) in Forks (Columbia River Basin) as observed and simulated by the CART and analog methods from the observed SLP field and from the different model runs in winter and sumer.

	Winter		Summer	
Observ	15.1		2.3	
	CART	analog	CART	analog
NMC	14.9	14.4	2.6	2.1
MPI	14.6	15.6	2.4	1.5
MPI $2xCO_2$	14.2	15.9	2.4	1.5
GFDL	16.1	14.9	2.1	1.7

It can be seen that the differences between the real and simulated mean precipitation are well within the observed interannual variability for both models. However, it should be noted that a completely random resampling from the observations would have yielded the right mean precipitation and therefore these numbers alone do not demonstrate the goodness of the precipitation generator. With respect to the $2xCO_2$ MPI run, no significant deviations were found from the 1xCO2 experiment in terms of mean

precipitation.

The probability density functions of daily precipitation for Forks (West Coast) as derived from the observations and generated from the observed and simulated SLP fields are shown in Fig 11. All probability distributions are in good agreement but again this is not necessarily be due to the skill of the method.

Fig. 12 shows the log-survivor functions of the storm interarrival times for Forks derived from the historical precipitation data, and by applying the precipitation generator to the daily SLP fields observed (NMC) and simulated by the three GCM runs. The log-survivor functions show that dry periods tend to last longer in the observations than in all model runs, in winter as well as in summer. Since there is no systematic under- or overestimation of the weather state lifetimes in the model simulations (see Fig. 10), this result indicates that there is some persistence in the precipitation process that is not properly captured by this precipitation generator. This reasoning is supported by the fact that the storm interarrival times generated with the historical SLP data as input variables are also shorter than the actual storm interarrival times, consistent with the findings of Hughes et al (1993). In winter, for all data sets the storm interarrival times are generally shorter at Forks than at West Glacier (not shown), a station located in the interior. Since weather state 1 (wet state) and weather state 2 (dry state) are mainly associated with wet or dry days, respectively, at all stations simultaneously, this difference in the behavior of the log-survivor functions can be traced to weather state 3 (hybrid state). This also explains why the GFDL model produces shorter storm interarrival times than the MPI model: The GFDL model simulates shorter series of weather state 3 (hybrid state), and weather state 2 (dry state) has a fairly low probability in both models.

In the summer months the storm interarrival times are similar in all stations (only results for Forks are shown in Fig 12). This should be due to the fact that in summer only two weather states have been identified, an "all- dry" state and an "all-wet" state. Furthermore, both models behave nearly equally with respect to the storm interarrival times. This is easily explained since the two models simulate very similar lifetimes of the dry weather state (Fig. 10).

6.2 Precipitation Generator Based on Analog Method

CART analysis is a sound classification scheme that also provides a physical interpretation of the resulting weather types. However the failure of the rainfall generator based on CART to replicate the observed storm interarrival times could limit the application of this method. Possible reasons for this shortcoming may lie in the dependence of rainfall occurrence on the precipitation amounts in previous days (Hughes et al., 1993; Bardossy and Plate, 1991). Another possibility is that precipitation events depend more strongly on the evolution of the atmospheric circulation in previous days than assumed in the CART analysis.

In this section an alternative precipitation generator will be presented to investigate this second possibility. Given an SLP field simulated by a GCM experiment the idea is to find in the daily observations the closest possible SLP field and then take for the simulated precipitation the observed precipitation on the day so identified. This is the well-known analog method described in the literature (Lorenz, 1969) but we will use it here with a slight modification proposed by Barnett and Preisendorfer (1978). Instead of comparing directly the simulated and the possible analog SLP fields, both are projected onto the five leading EOFs (in our case 5 EOFs) derived from the observations. The "distance" between them is then calculated based on their coordinates in this new basis. In this way it is expected that a part of the noise present in the daily SLP fields will be filtered out. Another advantage is again that anomaly fields may be used, thus removing the possible bias in the mean circulation simulated by the GCMs.

As with the CART-based precipitation generator, this method was also checked using the observed SLP fields as input. (In this case, to avoid any artificial skill, the "analog" circulation was selected from years other than the one being simulated). The generated storm interarrival times

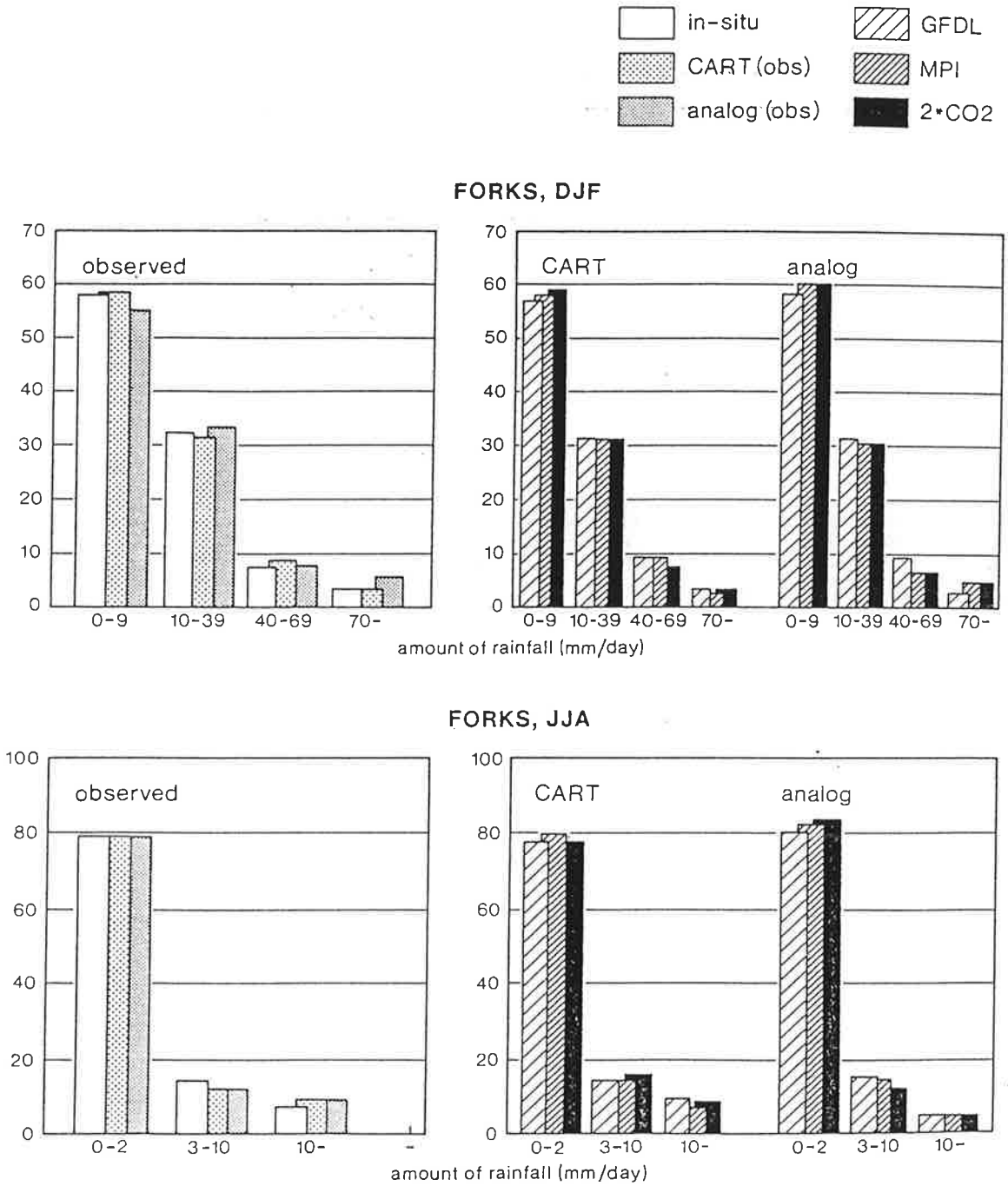

Figure 11. Daily rainfall (mm/day) probability distribution as observed and generated by the CART and ANALOG methods from the NMC analysis and from different model runs in winter (DJF) and summer (JJA): a) Forks (West Coast); b) Hightstown (East Coast).

Figure 11 (cont)

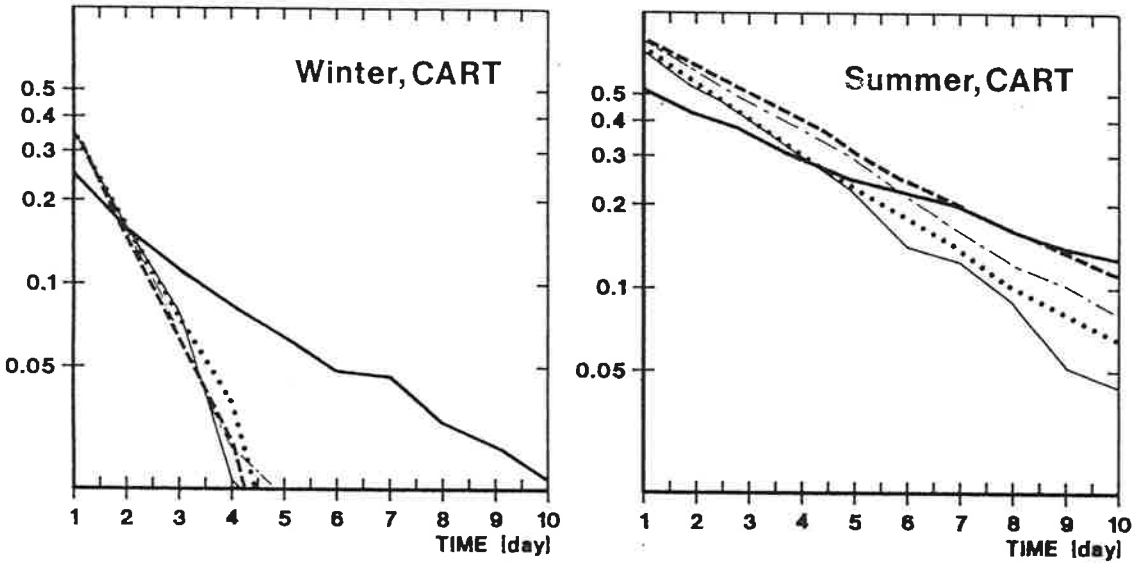

Figure 12. Log-survivor functions of the storm interarrival times in Forks (West Coast) in winter (DJF) and (JJA) as observed and generated with the CART and ANALOG methods from the NMC analysis and the different model runs: —— Observations; .... NMC; —— GFDL; --- MPI;- - - MPI ($2xCO_2$).

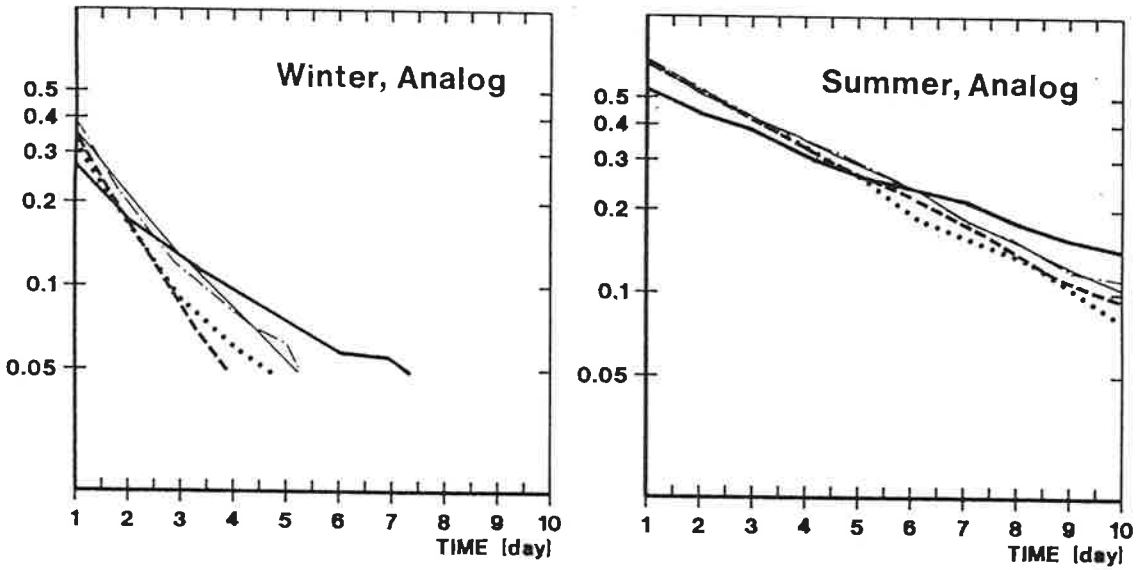

Figure 12 (cont): —— Observations; .... NMC; —— GFDL; --- MPI;- - - MPI ($2xCO_2$).

(not shown) tended still to be too short when compared with the historical precipitation data. As a further refinement to this method, the analog circultion was sought not just by comparing single SLP fields but comparing the evolution of the circulation in the previous four days, i.e the circulation in the present day and in the previous four days was compared to all the historical five-day segments and the most similar of them (also in terms of the EOFs coordinates)was taken as the analog. Then, the observed precipitation for the fifth day was ascribed to the circulation pattern in question

For brevity only the results results of this analogue-based method for Forks (West Coast) and Hightstown (East Coast) are presented.

Table 6.Mean rainfall (mm/day) in Hightstown (East Coast) as observed and simulated by the analog method from the observed SLP field and from the different model runs in winter (DJF)and summer (JJA).

	Winter	Summer
Observed	2.9	3.4
	analog	analog
NMC	2.8	3.7
MPI	3.0	3.7
MPI(2xCO_2	2.2	3.4
GFDL	2.8	3.9

Whereas the generated mean precipitation (Table 5 and 6) and probability density functions (Fig 11) do not deviate significantly from the results of the "one-segment" analog method, the log-survivor functions of the storm interarrival times (Fig. 12 and 13) are more similar to the ones derived from the observed precipitation data.

However, part of the apparent improvement might be spurious. Assume for simplicity that there is no time autocorrelation in the atmospheric circulation and that the analog for day d was found to be day k using both methods. Then, the probability that the analog for day d+1 lies in the surroundings of day k is greater in the "five-day-segment" method, (since only 20 percent of the information is new), than in the "one-day-segment" method. Therefore, the simulated storm interarrival times would artificially resemble those observed without necessarily implying that the method is representing the rainfall process better. To check how strong this problem can be in ourcase, consider Figure 14. It shows the probability that the analogs of day d and day d+n are separated exactly by n days, for the "one-day-segment", five-day-segment" and "ten-day-segment" methods in DJF in the North Pacific-American sector. It can be seen that these probabilities grow with increasing segment length, as expected, but they are only moderately high for a separation of one day. We believe, based on this analysis, that the persistence of the precipitation process may be better captured by weather generators that take into account the evolution of the daily SLP fields and that CART analysis using information from the SLP in the, roughly five previous days, would improve the results. However this would require considerably longer computer times, since the computational requirement grows exponentially with the number of input variables.

7. Conclusions

The ability of two GCMs to replicate selected regional features of the lower atmosphere circulation has been investigated and compared with historical data. In general, both of the GCMs are reasonably successful in simulating the major features of the observed mean circulation. For instance, both models reproduce qualitatively the quasi-permanent anticyclones over the Pacific and Atlantic Oceans in summer and the Aleutian and Icelandic Lows in winter, although in some cases the exact position and intensity of these features are misrepresented. The models also reproduce quite well the leading patterns of daily SLP variability on these regional scales, although some improvement is still necessary. In general the GFDL model shows a greater variability than the observations, whereas the MPI model is usually less variable. It is not obvious if this fact is related to the different ocean representation in these models, since other authors have found no significant differences in a GCM variability in experiments performed with fixed or varying SSTs

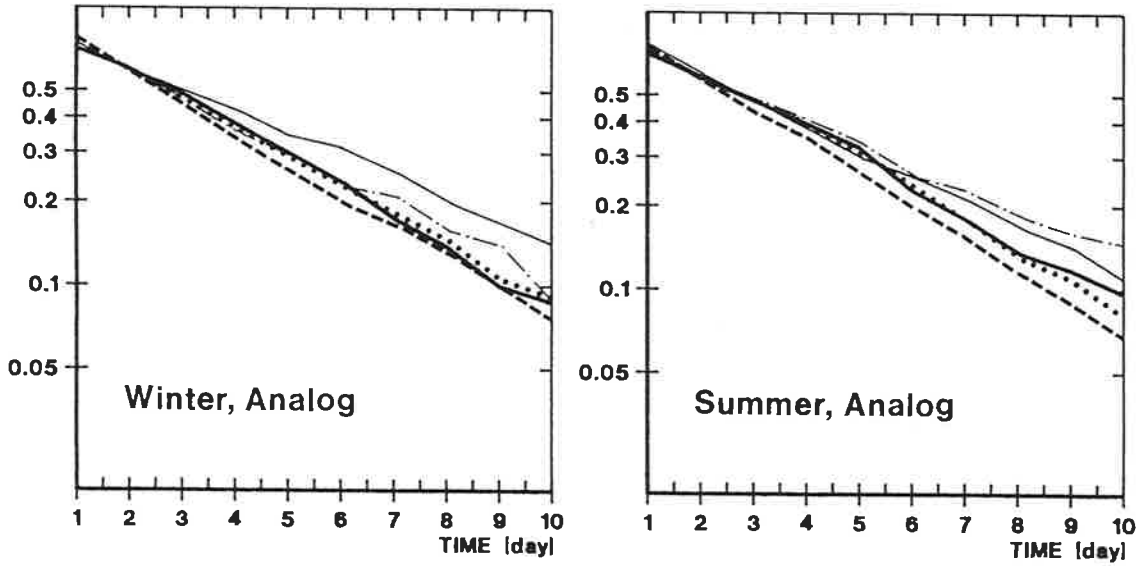

Figure 13. Log-survivor functions of the storm interarrival times in Hightstown (East Coast) DJF and JJA as observed and generated with the ANALOG method from the NMS analysis and from the different model runs:
—— Observations; .... NMC; —— GFDL; --- MPI;- - - MPI ($2xCO_2$).

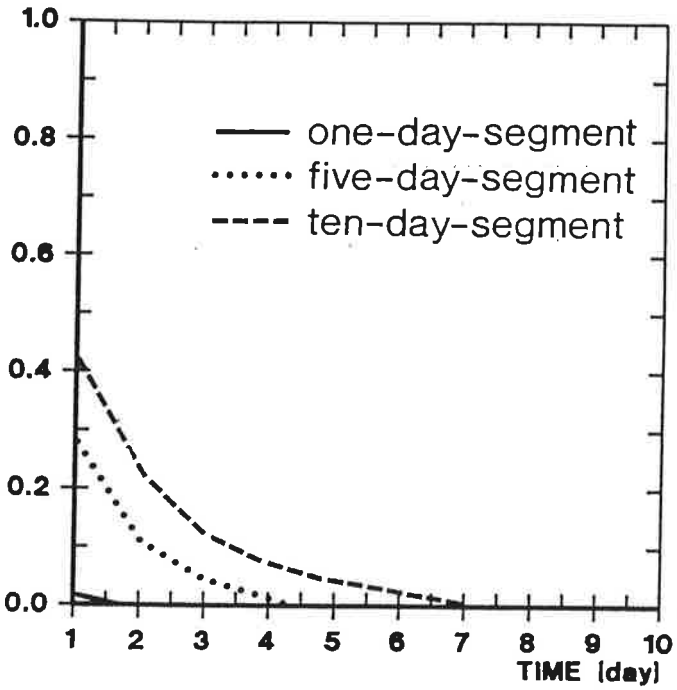

Figure 14. Probability that the anoalogs chosen for day d and day plus n (n from 1 to 10 days) are separated by exactly n days in DJF in the Pacific-North American sector for the "one-day-segment", "five-day-segment" and "ten-day-segment" methods.

(Chervin, 1986).

A CART classification scheme based on the daily SLP anomaly field and station precipitation data was applied to identify the weather states that are most strongly associated with the presence/absence of precipitation at those stations. For the winter season, a reasonable set of weather states was identified for the Columbia River basin. In the summer season only the stations that are located near the coast could be used to classify the daily large-scale SLP fields, indicating that precipitation events in the interior of the Columbia basin in summer not as dependent on the large-scale atmospheric circulation as in winter.

For the East Coast of the U.S., the situation is more complicated and it is virtually impossible to find any classification of weather states that could be meaningful for more than two stations. The East Coast precipitation seems to be coherent only at fairly short spatial scales. This would impose serious difficulties, for instance, when trying to assess future climate changes from the simulations of current low resolution climate models, since each area might react differently to changes in the large-scale circulation patterns.

In the cases when a set of weather states could be found, the GCM simulations were quite successful in reproducing the observed weather state occurrence probabilities. Although the GCM results have been corrected for the bias in their simulated long-term mean, their internal variability was not manipulated, so that GCMs show some skill in simulating the weather types. Some discrepancies were found in the log-survivor functions of the weather states, but there was no systematic bias, indicating that this behavior depends on the particular dynamics of each model.

A stochastic precipitation generator developed by Hughes at al. (1993) and based on CART analysis was applied to the historical and simulated SLP fields. The results so obtained were compared to a simpler stochastic generator based on an analog method. It was found that both methods were able to reproduce the low-frequency precipitation variability and the probability distribution of daily precipitation amounts.

The storm interarrival times simulated by the CART-generator were generally shorter than the observed ones (a result also found by Hughes et al., 1993), whereas the analog-generator was able to produce interarrival times closer to the observations, although they still tend to be too short. This behavior of the CART generator may be related to its use of SLP information from the present and previous day only, whereas the analog method uses the previous five days. Furthermore the CART-generator in its present form cannot easily handle the time evolution of the SLP field since each node of the decision tree is split based on the value of a single variable. Further refinement of this precipitation generator might perhaps be achieved by simultaneously including in the analysis information of the present and several previous days at the expense of increasing computer time.

With respect to the changes in precipitation caused by a CO_2 doubling, small differences were found between the MPI control run and the $2xCO_2$ experiment. The reasons for this result are probably the low climate sensitivity of the MPI model in comparison with other models (Houghton et al 1990) and that the signal-to-noise ratio in the SLP is usually lower in altered $2xCO_2$experiments (Barnett, 1991).

References

Barnett, T.P., 1991: An attempt to detect the greenhouse signal in transient GCM simulation. In Greenhouse-Gas induced Climate Change: A critical appraisal of simulations and Observations. M.E, Schlesinger (Ed.), 559-568

Barnett, T., and R. Preisendorfer, 1978: Multifield analog prediction of short-term climate fluctuations using a climate state vector. J. Atmos. Sci.35, 1771-1787.

Bardossy, A., and E.J. Plate, 1991: Space-time modeling for daily rainfall using atmospheric circulation patterns. Water Resources Res. 28, 1247-1259.

Barros A.P., and D.P. Lettenmaier, 1993: Multiscale aggregation and disaggregation of precipitation for regional hydroclimatological studies. In Yokohama Assembly Proceedings of the International Association of Hydrological Sciences.

Breiman, L., J.H. Friedman, R.A. Olsen, and J.C. Stone, 1984: Classification and regression trees. Wadsworth, Monterrey.

Chachine, M. T., 1992: The hydrological cycle and its influence on climate. Nature 359, 373-380.

Chervin, R.M.,1985: Interannual variability and seasonal climate predictability. J. Atmos. Sci. 43, 233-251.

Cubasch, U., K. Hasselmann, H. Hoeck, E. Maier-Reimer, U. Mikolajewicz, B.D. Santer, and R. Sausen, 1992: Time-dependent greenhouse warming computations with a coupled ocean-atmosphere model. Climate Dynamics 8, 55-59.

Giorgi, F., 1990: Simulation of regional climate using a limited area model nested in a general circulation model. J. Climate 3, 941-963.

-----, and L.O. Mearns, 1991: Approaches to the simulations of regional climate change: a review. Rev. Geophys. 29, 191-216 .

Grotz,S., M.C. MacCracken, 1991: The use of general circulation models to predict regional climate change. J. Climate 4, 286-303.

Houghton, J.T.,G.J. Jenkins, and J.J. Ephraums (eds), 1990: Climate change.The IPCC Scientific Assessment. Cambridge University Press.

Hughes, J.P., D.P. Lettenmaier, and P. Guttorp, 1993: A stochastic approach for assessing the effect of changes in regional circulation patterns on local precipitation Accepted for publication, Water Resources Res.

Karl, T.R., W.-C. Wang, M.E. Schlesinger, R.W. Knight, and D. Portman, 1990: A method of relating General Circulation Model simulated climate to the observed local climate. Part I: Seasonal statistics. J. Climate 3, 1053-1079.

Klein, W.H., and H. Bloom, 1988: An operational system for specifying monthly precipitation amounts over the United States from the field of concurrent mean 700-mb heights. Weather and Forecasting 4, 51-60.

------, and B. Whistler, 1990: Specification of monthly mean anomalies of fire weather elements in the United States. Agricultural and Forest Meteor., 56, 145-172.

Lorenz, E.N. 1969: Atmospheric redictability as revealed by naturallyocurring analogs. j. atmps sci. 26, 636-646

Mass, C.F., H.J. Edmon, H.J. Friedman, N.R. Cheney, and E.E. Recker, 1987: The use of compact discs for the storage of large meteorological and oceanographic data sets, Bull. Am. Meteorol. Soc., 68(12), 1556-1558.

Preisendorfer, R., 1988: Principal components analysis in meteorology and oceanography. Elsevier, Amsterdam.

Rind, D.,C. Rosenzweig, and R. Goldberg, 1992: Modeling the hydrological cycle in assessment of climate change. Nature 358, 119-122.

Roeckner E., L Dumenil, E. Kirk , F. Lunkeit, M. Ponater, B.Rockel, R. Sausen and U. Schlese, 1989: The Hamburg version of the ECMWF model (ECHAM). GARP Report No. 13, WMO, Geneva, WMO/TP No. 332.

Shabbar, A., K. Higuchi, and K. Knox, 1990: Regional analysis of NorthernHemisphere 50 kPa geopotential height from 1946 to 1985. J. Climate 3, 543.

Thomas, G., and A. Henderson-Sellers, 1991: An evaluation of proposed representations of sub-grid hydrologic process in climate models. J. Climate 4, 898-910.

v. Storch, H., E. Zorita, and U. Cubasch, 1993: Downscaling of climate change estimates to regional scales: application to winter rainfall in the Iberian Peninsula. Journal of Climate, in press.

Wallis, J.R., and D.P. Lettenmaier, 1991: A daily hydroclima tologicaldata set for the continental United States. Water Ressources Research 27, 1657-1663

Wigley T.M.L., P.D. Jones, K.R. Briffa, and G. Smith, 1990: Obtaining sub-grid scale information from coarse-resolution general circulation model output J. Geophys. Res. 95, 1943-1953.

Wilson, L.L., D.P. Lettenmaier, and E. Skyllingstad, 1992: A multiple stochastic daily precipitation model conditional on large-scale atmospheric circulation patterns. J. Geophys. Res. 97, 2791-2809 .